

**CHARACTERIZATION OF SPONTANEOUS, JUVENILE-TYPE GRANULOSA
CELL TUMOURS FROM SWR MICE**

by

© Clare Lewis

A Thesis submitted to the

School of Graduate Studies

in partial fulfillment of the requirements for the degree of

Master of Science

Faculty of Medicine

Memorial University of Newfoundland

May 2018

St. John's

Newfoundland and Labrador

Table of Contents

Abstract	i
Acknowledgements	ii
List of Tables	iii
List of Figures	iv
List of Abbreviations	v
List of Appendices	viii
1.0 Introduction: Overview of the female ovary and its reproductive functions	1
1.1 Overview of sex specification of the mammalian gonad	3
1.1.1 Sex chromosomes dictate gonadal sex.....	3
1.1.2 Testis development from the bipotential gonad.....	5
1.1.3 Ovary development from the bipotential gonad	7
1.2 Ovarian Physiology Over the Lifespan	10
1.2.1 The pre-pubertal ovary	10
1.2.2 Puberty and the establishment of reproductive cyclicality.....	13
1.2.3 The post-menopausal ovary.....	18
1.3 Ovarian Tumourigenesis	19
1.3.1 Granulosa cell tumours.....	19
1.3.2 AGCT of the ovary.....	20
1.3.3 JGCT of the ovary.....	22
1.3.3.1 COV434 human GCT cell line.....	24
1.3.3.2 SWR mouse model for early-onset GCT	28
1.4 Experimental Rationale	33
1.5 Hypothesis and Research Objectives	34
1.5.1 Hypotheses:	34
1.5.2 Research Objectives	34
2.0 Materials and Methods	35
2.1 Animal Husbandry and Protocol Approvals	35
2.2 Tissue Sample Collection	35
2.3 COV434 Cell Culture	37
2.4 COV434 Sample Collection	37
2.5 Tissue Fixation	38
2.5.1 Hematoxylin and Eosin Staining & Brightfield Imaging	38
2.5.2 Tissue collection for immunohistochemistry (IHC).....	38
2.6 Brightfield Imaging	39
2.7 BCA Protein Assay	39
2.8 Immunoblotting	40
2.10 Immunohistochemistry	45
2.11 Statistics	48

3.0 Results	49
3.1 Immunoblotting Analysis.....	49
Cyp19a.....	49
Fshr	50
Egfr	50
Esr2.....	52
Foxl2.....	52
Sox9.....	57
3.2 Immunohistochemical Analysis.....	60
4.0 Discussion.....	64
Overview	64
4.1 SWR mouse strain GC tumours and the normal ovarian condition	65
4.2 The normal ovary and a model human JGCT cell line, COV434.....	73
4.3 The Mouse GC tumour and a model human GCT cell line, COV434.....	74
5.0 Summary	78
6.0 Future Directions.....	79
7.0 References.....	81
Appendix A Copyright Permissions	90
Appendix B Summary of inventoried samples.....	93

Abstract

Granulosa cell tumours (GCTs) are a subtype of ovarian cancer derived from the granulosa cells (GC) surrounding the oocytes. The SWR mouse is a well defined model for juvenile-type GCTs in terms of endocrinology, genetics and malignancy. GCTs appear spontaneously in SWR-derived female mice at puberty, characterized by rapid, benign growth followed by a malignant transition after 6-10 months in approximately half of the tumour-bearing population. Our aim is to characterize the protein expression profile of early GCTs, normal ovaries and the human COV434 JGCT cell line to determine if protein expression differences can help identify the mechanism of tumourigenesis. This was accomplished using immunoblotting to define the protein expression profile of mouse primary GCTs, normal, whole ovaries and human COV434 cell lysates. Protein lysates from the early GCTs were positive for expression of Cyp19a, Fshr, Egfr, Esr2, Foxl2 and Sox9 proteins, with significant downregulation of Esr2 and significant upregulation of Egfr in GCTs relative to both normal ovaries. A further evaluation of Sox9 was done by immunohistochemistry, which confirmed a proportion of cell specifically express Sox9, although the cellular identity is not conclusively that of GCT cells. Protein lysates from the COV434 cell line compared to the mouse GCTs were also positive for expression of Cyp19a, Fshr, Egfr, Esr2 and Foxl2 proteins, with significant upregulation of Cyp19a, significant downregulation of Egfr and Esr2, and no Sox9 protein expression. A further evaluation of Sox9 was done by immunohistochemistry and confirmed its expression in GCTs. The protein profile of GCTs, as compared to normal ovaries and a human representative cell line will provide a basis for future studies of juvenile-type GCT genetics, biology and therapy.

Acknowledgements

First I would like to thank my supervisors, Dr. Ann Dorward and Dr. Jules Doré, for allowing me this opportunity and learning experience and for guiding and teaching me to be a better scientist. Both Dr. Dorward and Dr. Doré provided me with valuable opportunities and experiences that helped to further my academic career. I look forward to their further guidance as I complete my PhD program over the next four years as members of my committee.

I would like to thank my committee member Dr. Laura Gillespie. The helpful and valuable comments she always provided and the questions she asked helped me to learn to think more critically and were very much appreciated.

Thank you to all the members of the Dorward and Doré labs, who provided me with technical help, as well as moral support throughout my degree: Ed Yaskowiak, Zoha Rabie, Krista Squires and others. A special thanks to Kerri Smith for always helping when needed and for being a great friend.

I would like to acknowledge the funding agencies who supported me throughout my degree: the Canadian Institutes of Health Research (CIHR), Newfoundland and Labrador's Department of Innovation, Trade and Rural Development, the Janeway Foundation and Memorial University of Newfoundland's School of Graduate Studies. Thank you as well to the Faculty of Medicine's Office of Research and Graduate Studies, the Medical Graduate Student Society and CIHR for providing travel funds and awards.

Last but certainly not least; I would like to extend my greatest thanks to all my family and friends, especially Wayne Graves and my parents who have supported me throughout my program. The love and support you have shown will never be forgotten.

List of Tables

Table 1.1 Genes involved in the development of the bipotential gonad and male/female sex determination pathways (Table adapted from She & Yang, 2014).....	8
Table 1.2 Comparison of adult type and juvenile type GCTs in humans.....	25
Table 1.3 Comparison of KGN, COV434 cell lines and the SWR mouse model.....	27
Table 2.1 Detailed list of antibodies used in immunoblotting and IHC.....	43
Table B.1 Summary of normal ovarian samples from SWR background mice analyzed by immunoblotting.....	92
Table B.2 Summary of GCT samples from SWR background mice analyzed by immunoblotting.....	93
Table B.3 Summary of cell lysate samples from the human cell line COV434 analyzed by immunoblotting.....	94
Table B.4 Summary of tissues from mice for analysis by IHC.....	94

List of Figures

Figure 1.1 Anatomy of the ovary	2
Figure 1.2 The bipotential gonad and determination of sex.....	4
Figure 1.3 Ovarian folliculogenesis	12
Figure 1.4 The hypothalamic-pituitary-gonadal axis.....	15
Figure 1.5 The two-cell, two-gonadotropin theory of hormone production and regulation in follicles.....	17
Figure 1.6 Histology of normal whole ovaries (A) and granulosa cell tumours (B) from SWR mice	30
Figure 1.7 Gross GCT specimen from SWR mouse.....	31
Figure 3.1 Quantitative representation and immunoblot analysis of Cyp19a	51
Figure 3.2 Quantitative representation and immunoblot analysis of Fshr.....	53
Figure 3.3 Quantitative representation and immunoblot analysis of Egfr.....	54
Figure 3.4 Quantitative representation and immunoblot analysis of Egfr.....	55
Figure 3.5 Quantitative representation and immunoblot analysis of Esr2.....	56
Figure 3.6 Quantitative representation and immunoblot analysis of Foxl2.....	58
Figure 3.7 Quantitative representation and immunoblot analysis of Sox9	59
Figure 3.8 IHC of normal gonad condition.....	61
Figure 3.9 IHC of JGCTs from SWR background mice	62

List of Abbreviations

°C	degrees Celsius
α	alpha
β	beta
μg	microgram
μL	microliter
17 β -HSD	17 β -hydroxysteroid dehydrogenase
3 β -HSD	3 β -hydroxysteroid dehydrogenase
AGCT	adult granulosa cell tumour
AMH	anti-Müllerian hormone
ANOVA	analysis of variance
Ar	androgen receptor protein
BME	β -mercaptoethanol
BPES	blepharophimosis-ptosis-epicanthus inversus syndrome
BRCA	BRCA, DNA repair associated
BSA	bovine serum albumin
Chr	chromosome
CO ₂	carbon dioxide
CTNNB1	beta-catenin
CYP11A1	cholesterol side-chain cleavage enzyme
CYP17A1	cytochrome P450 17A1
Cyp19a	cytochrome P450, family 19, subfamily a, polypeptide 1
d	days
DHEA	dehydroepiandrosterone
DHT	dihydrotestosterone
DMEM	Dulbecco's modified eagle medium
DNA	deoxyribonucleic acid
dpi	dots per inch
E	embryonic day
E ₂	17 β - estradiol
Egfr	epidermal growth factor receptor
Esr1	estrogen receptor 1
Esr2	estrogen receptor 2
FBS	fetal bovine serum
FCS	fetal calf serum
Fgf9	fibroblast growth factor 9
Foxl2	forkhead box l2
Fsh	follicle stimulating hormone
Fshr	follicle stimulating hormone receptor
g	gravity force
g	gram
Gata4	GATA binding protein 4
GC	granulosa cell
GCT	granulosa cell tumour
<i>Gct</i>	Granulosa cell tumour susceptibility genetic locus

GF	growth factor
GnRH	gonadotropin-releasing hormone
Ht	height
H	hormone
h	hour
H&E	hematoxylin and eosin
hCG	human chorionic gonadotropin
HCl	hydrochloric acid
HITES	hydrocortisone, insulin, transferrin, estradiol and sodium selenite
HPG	hypothalamic-pituitary-gonadal
HRP	horseradish peroxidase
IHC	immunohistochemistry
IVF	invitro fertilization
JGCT	juvenile granulosa cell tumour
JGCTT	juvenile granulosa cell tumour of the testis
kDa	kilodaltons
L	length
l	liters
LH	luteinizing hormone
LHR	luteinizing hormone receptor
LHX9	LIM homeobox protein 9
mA	milliamps
Mb	megabase
min	minute
mL	milliliter
mm	millimeter
mM	millimolar
M	molar
mm ³	millimetres cubed
mRNA	messenger ribonucleic acid
NaCl	sodium chloride
nm	nanometer
NR	nuclear receptor
NS	not significant
P ₄	progesterone
PBS	phosphate buffered saline
PMSF	phenylmethanesulfonyl fluoride
POF	premature ovarian failure
PVDF	polyvinylidene fluoride
RIPA	radioimmunoprecipitation assay
RSPO-1	r-spondin 1
RT-PCR	reverse transcriptase polymerase chain reaction
SCST	sex cord-stromal tumour
SDS	sodium dodecyl sulfate
SF1	steroidogenic factor 1
SM	signaling molecule

Sox9	SRY box9
SRY	sex-determining region of Chr Y
StAR	steroidogenic acute regulatory protein
T	testosterone
TBST	TRIS buffered saline with Tween-20
TC	thecal cell
TF	transcription factor
TGF β	transforming growth factor beta
TP53	tumour protein p53
V	volts
W	width
wk	week
WNT4	wingless-type MMTV integration site family member 4
WT1	Wilms' tumour 1
yr	year

List of Appendices

- | | |
|------------|---------------------------------------|
| Appendix A | Copyright permissions |
| Appendix B | Summary of inventoried tissue samples |

1.0 Introduction: Overview of the female ovary and its reproductive functions

The ovary is the female gonad or reproductive gland of many species (Figure 1.1). In mammals it is a paired organ residing in the abdominal cavity and has two main functions: the production of oocytes, the female germ cells, and the production of steroid and protein hormones, primarily the steroid hormones estrogen (E_2) and progesterone (P_4). A specific population of somatic cells called granulosa cells (GCs) nurtures the female germ cell, the oocyte, in the female gonads. GCs provide support to the developing oocytes in the context of individual ovarian follicles and are necessary for their maturation into competent gametes (Adashi & Leung, 1993).

In humans, puberty is defined by the activation of ovarian cyclicity and the beginning of female reproductive potential. Puberty marks the onset of the production of sex hormones by the ovary, which in turn allows for controlled ovulation of oocytes competent for fertilization and embryonic development. At the end of reproductive life, there is a normal decline in the number of available oocytes able to mature for ovulation (Adashi & Leung, 1993). This can be attributed to there being a limited starting pool of follicles in the fetal ovary, leading to a perimenopausal period of reproductive decline (Tingen *et al.*, 2009). This marked and natural reproductive senescence is referred to as menopause in humans, a time when ovulation ceases and hormone production is drastically reduced by the ovary. Aside from the natural reproductive senescence, disruptions in normal development and ovarian function can arise from genetic variations

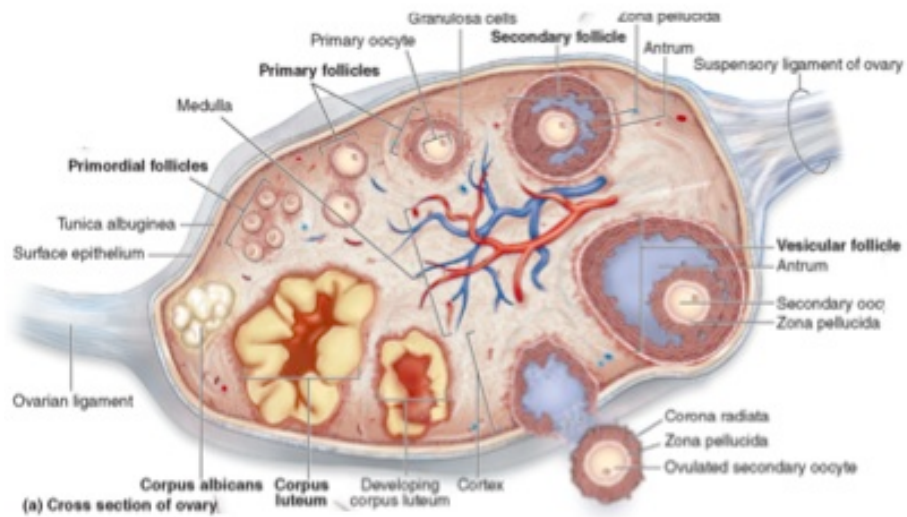


Figure 1.1 Anatomy of the ovary

The anatomy of the human ovary is complex with many components. A layer of surface epithelium surrounds the ovary, which has a central medulla and an outer cortex populated with follicles. The post-pubertal, pre-menopausal ovary contains follicles at various stages of the maturation cycle, including: primordial follicles primary and secondary follicles, antral follicles and mature (vesicular) follicles ready for ovulation. The corpus luteum (CL) is a hormone-secreting collection of luteinized granulosa cells formed from post-ovulatory follicles, while the corpus albicans is an inactive remnant of a prior CL (Used with permission from McGraw-Hill).

leading to reduced fertility or pathological outcomes. These variations may be inherited germline mutations that are present in all cells of the body, or they may be acquired throughout the lifespan in a subset of cells, and therefore defined as somatic mutations. By understanding ovarian development, functioning and maintenance throughout the reproductive years of life, we can better understand how any genetic alterations, whether germline or somatic, contribute to aberrant ovarian function, specifically ovarian tumourigenesis, in both mice and humans.

1.1 Overview of sex specification of the mammalian gonad

1.1.1 Sex chromosomes dictate gonadal sex

During the early stages of embryogenesis, reproductive development has two potential fates: to follow the male pathway with specification of testes and development of the Wolffian ducts, or to follow the female pathway with specification of the ovary and development of the Müllerian ducts (Kobayashi and Behringer, 2003). The pathways of primary gonadal sex determination are initiated by gene expression from the mammalian X and Y sex chromosomes (Chr), with Chr XY inheritance establishing male development and Chr XX inheritance establishing female development. Following gonad specification, unique gonadal structures, supporting cells and sex hormones influence the production and development of the sex-specific germ cells, sperm in males and oocytes in females (Eggers *et al.*, 2014). Supporting somatic cells of the developing testis are named Sertoli and Leydig cells, while in the ovary they are named granulosa cells (GCs) and thecal cells (TCs), respectively (Windley & Wilhelm, 2015).

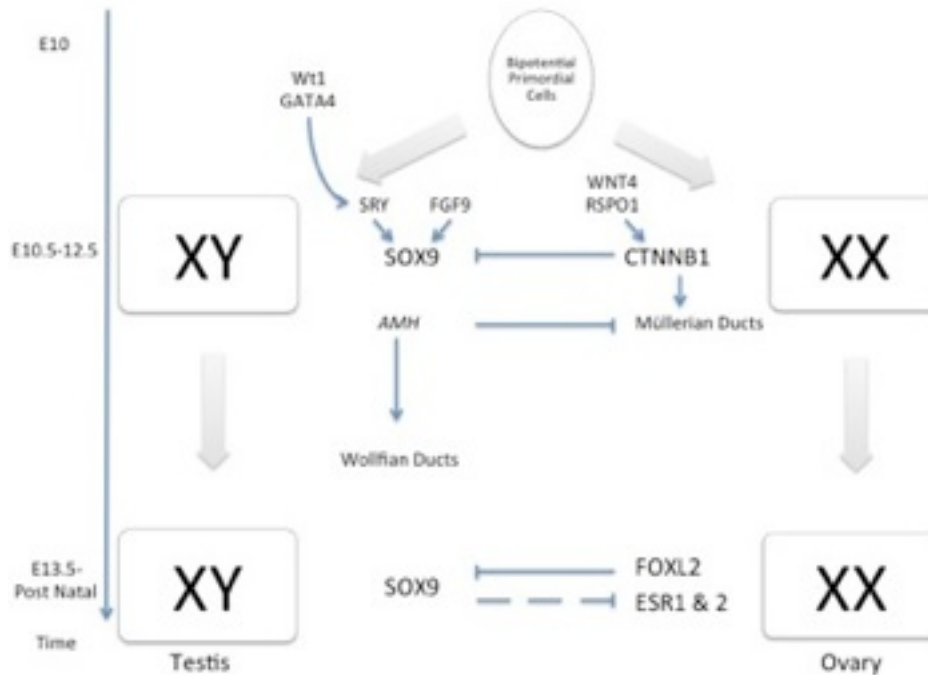


Figure 1.2 The bipotential gonad and determination of sex

In early sex determination, at approximately embryonic day (E) 10 in mice, primordial cells have the potential to develop into either the male gonad (XY) or the female gonad (XX). Wt1 and GATA4 promote the expression of SRY. SRY acts to stimulate SOX9, which prompts the male gonad to develop (E10.5-12.5). FGF9 also acts in male gonad development to maintain the expression of SOX9. During male gonad development, AMH is expressed which causes the regression of the female Müllerian ducts and in the presence of androgens the formation of the Wolffian ducts. In the absence of SRY and the presence of CTNNB1, a pathway that is stimulated by WNT4 and RSPO-1, the female gonad develops (E10.5-12.5). After the ovary has developed (~E13.5), CTNNB1 expression declines and other factors, including FOXL2, ESR1 and ESR2 act to continually repress SOX9 and maintain the ovarian phenotype. CTNNB1 also promotes the formation of the Müllerian ducts in the absence of AMH.

The fate of the bipotential gonad is established early in fetal development. The, bipotential gonad (Figure 1.2) persists up to day E10 in mice and up to gestational week (wk) 9 in humans (Wunsch & Schober, 2007). Primary sex determination subsequently takes place between E10.5-12.5 in mice and gestational wk 9-12 in humans, involving several key transcription factors and a nuclear receptor network that regulate the development of the bipotential gonad into its sex-specific form (Wunsch & Schober, 2007).

1.1.2 Testis development from the bipotential gonad

The male pathway and testis development from the bipotential gonad proceeds with Chr XY inheritance. Chr Y is a relatively small chromosome comprised of only 183 protein coding genes in the mouse and 63 in humans (GRCh38.p10: Ensembl Release 90). One of the most influential genes on Chr Y in mice and men is the *Sex-determining Region of Chr Y (SRY)* gene. This gene is initially regulated by the cooperative expression of the transcription factors Wilms' tumour 1 (WT1) and GATA binding protein 4 (GATA4; Tanaka *et al.* 2014). The expression of *SRY* occurs at approximately E11.0 in mice and as early as 41 days post-conception in the cells of the genital ridge in humans (Hanley *et al.* 2000; Tanaka *et al.* 2014). The expression of *SRY* is important in the early stages of gonad development to trigger a signaling cascade that leads to the recruitment of *SRY-box 9 (SOX9)*-expressing pre-Sertoli cells and subsequently inhibits ovarian differentiation (Tanaka *et al.* 2014). Following its activation by *SRY*, *SOX9* expression is maintained in the developing testis by Fibroblast Growth Factor 9 (FGF9) along with other factors. The expression of *SOX9* helps to sustain testis development by acting in a positive feedback loop, as well as acting to promote Sertoli cell proliferation

(Wilhelm *et al.*, 2007; Tanaka *et al.* 2014). Table 1.1 outlines these genes and others involved in the development and determination of the bipotential gonad, as well as describing phenotypes involved with loss of function of these genes. Using mouse as a model organism, when *Sry* loss of function occurs in Chr XY gonads, male-to-female sex reversal is observed; conversely, when *Sry* is overexpressed in the Chr XX gonads, female-to-male sex reversal occurs (Koopman *et al.* 1989). A similar result arises when there is loss of function in the *Sox9* gene, and male-to-female sex reversal ensues, with abnormal development and differentiation of the Sertoli cells (Huang *et al.* 1999). The outcomes of these loss-of-function mutations in the *Sry* and *Sox9* genes demonstrate their importance in normal testis development.

The development of the mature Sertoli cells regulates the formation and differentiation of the Leydig cells, which produce the male sex hormone, Testosterone (T; Sekido *et al.* 2012). The production of T and subsequently dihydrotestosterone by the Leydig cells then act as ligands for the androgen receptor (Ar) to develop secondary sex characteristics such as the external genitalia (Tanaka *et al.* 2014; Sekido *et al.* 2012). The expression of *SOX9* by the Sertoli cells also leads to *Anti-Müllerian Hormone (AMH)* or *Müllerian Inhibiting Substance (MIS)* being expressed to cause the regression of the Müllerian ducts in female embryos (Koopman *et al.*, 2001), in turn allowing for the male counterpart, the Wolffian ducts. The Wolffian ducts will later form components of the male reproductive system, including the epididymis and seminal vesicles (Wilhelm *et al.*, 2007). These components, along with the Sertoli cells and T-producing Leydig cells will later aid in the differentiation and maturation of the germ cells into mature sperm (Tanaka *et al.* 2014).

1.1.3 Ovary development from the bipotential gonad

It was initially thought that the female (or ovarian) fate of gonad development was the default pathway when the sex chromosomes and genes necessary for male development were not present. This hypothesis was developed by investigating the fate of the population of supporting cells in the developing gonad using several different models including transgenic and mutant mice, cultured gonads, and transplanted and chimeric gonads (McLaren, 1991). These studies concluded that in supporting cells where the male-determining gene was expressed in a sufficient quantity, pre-Sertoli cells would develop and therefore proceed to the testis pathway. When the male-determining genes was not expressed in a sufficient number of supporting cells, or was not expressed at the appropriate time in development, the cells would differentiate into pre-follicle cells, now referred to as GCs (McLaren, 1991). This hypothesis has changed over time as a reflection of research progress. Forkhead box L2 (*FOXL2*), a transcription factor that belongs to the forkhead/winged helix transcription factor family, was determined to be expressed in the female gonad in the early somatic cells, it was subsequently considered to be the female determining gene, similar to *SRY* and *SOX9* in the male pathway (Georges *et al.* 2013).

Ovaries that develop from the bipotential gonad are selected with Chr XX inheritance. Once the bipotential gonad has initiated the female sex determination pathway, the downstream signaling events important for female sex specification proceed. The activation of the Wingless-type MMTV integration site family member 4 (WNT) / β -catenin (CTNNB1) pathway, regulated by R-spondin 1 (RSPO-1) occurs between E10.5

Table 1.1 Genes involved in the development of the bipotential gonad and male/female sex determination pathways (Table adapted from She & Yang, 2014)

Gene	Protein Function	Phenotypes		Reference
		Human Syndrome (OMIM #)	Mouse Models	
<i>Gata4</i>	TF	615542	Failure in thickening of the coelomic epithelium, defective initial formation of genital ridge	Lourenco <i>et al.</i> , 2011
<i>Wt1</i>	TF	194080, 136680	Disruption of seminiferous tubule and somatic cell apoptosis, XY sex reversal	Gao <i>et al.</i> , 2006
<i>Sfl</i>	NR	273250	Delayed organization of male testis cord, failure in genital ridge formation	Reuter <i>et al.</i> , 2007
<i>Sry</i>	TF	400044, 400045	XY sex reversal; XX sex reversal	Koopman <i>et al.</i> , 1989
<i>Sox9</i>	TF	114290	Abnormal Sertoli cell differentiation, XY sex reversal; XX sex reversal	Huang <i>et al.</i> , 1999
<i>Amh</i>	H	400044	XY sex reversal	-
<i>Fgf9</i>	GF	400044	XY sex reversal	Jameson <i>et al.</i> , 2012
<i>Wnt4</i>	SM	158330	Failure in the formation of coelomic vessel and germ cell degeneration of the female reproductive tract, partial XX sex reversal	Yao <i>et al.</i> , 2004
<i>β-catenin</i>	TF	-	Partial XX sex reversal	Chassot <i>et al.</i> , 2008
<i>Rspo1</i>	GF	610644	Development of ovotestes, partial XX sex reversal	Chassot <i>et al.</i> , 2008
<i>Foxl2</i>	TF	110100	Premature ovarian failure, ablation of the primordial follicle pool, partial XX sex reversal	Uhlenhaut & Treier, 2006

*TF- Transcription Factor, NR- Nuclear Receptor, H- Hormone, GF- Growth Factor, SM- Signaling Molecule

and E12.5 in mice and 6 to 9 wks post-conception in humans. As well as being a key factor in the ovarian pathway, CTNNB1 also counteracts the male pathway by not only disrupting SOX9 but also acting to suppress the development of male-specific coelomic blood vessels, subsequently allowing the Müllerian ducts to become the female reproductive structures, including the oviducts, cervix and uterus, while the Wolffian ducts regress (Chassot *et al.*, 2008; Boyer *et al.*, 2010). Foxl2 along with Estrogen Receptor α (Esr1) and Estrogen Receptor β (Esr2) work to repress Sox9 and prevent the trans-differentiation of the ovary and its cells to the program of the male gonad (Uhlenhaut *et al.*, 2009); interestingly, studies looking at conditional inactivation of *Foxl2* results in GCs being trans-differentiated into Sertoli cells and an upregulation of Sox9 and other testicular genes (Tanaka *et al.* 2014). After the ovary is fully developed, Ctnnb1 expression declines and Foxl2, Esr1 and Esr2 function to maintain the ovarian phenotype (Figure 1.2).

When *FOXL2* mutations occur in the human population, they were found to be associated with blepharophimosis-ptosis-epicanthus inversus syndrome (BPES; OMIM 110100), which leads to eyelid malformations, and in some cases, premature ovarian failure (POF), but not ovary to testis sex reversal (Crisponi *et al.*, 2001). The absence of sex reversal in these patients indicates that although *FOXL2* is important in the development and functioning of the ovary, it is not solely responsible for early ovarian differentiation (Mork *et al.*, 2012).

In addition to studying humans, the mouse has been an excellent model to identify the primary determinants and maintenance factors that influence mammalian ovary specification, with strong translational value to the normal development and physiology

of the human ovary. Mice also present us with the opportunity to alter relevant and important genes to determine effects of aberrant function in the ovary. For instance, the mutation of *Foxl2* in mice has initiated POF and BPES (Uda *et al.*, 2004). These conditions, POF and BPES, have phenotype similarities in mice and the humans, including the disturbance of follicle formation and malformation of the eyelid, suggesting that a mouse model accurately mimics the human condition allowing for the investigation of ovarian function (Table 1.1).

1.2 Ovarian Physiology Over the Lifespan

1.2.1 The pre-pubertal ovary

The early ovary contains the entire pool of primordial follicles from the time of birth. In recent years, the exact origin of these follicles and their functions during reproductive life has been established. At birth, the ovary is filled with immature germ cells that later differentiate into mature germ cells or oocytes. The oocytes mature in the presence of supporting GCs as distinct follicles surrounded by a basement membrane (Figure 1.3).

The process by which follicles develop and are selected for ovulation is referred to as folliculogenesis. Folliculogenesis has three main stages: the formation of the primordial follicles, the recruitment of the primordial follicles into the pool of growing follicles, and lastly ovulation of the mature follicle with formation of the steroidogenically active corpus luteum post-ovulation (Edson *et al.*, 2009). The formation of the primordial follicles occurs at approximately gestational wk 18 to 22 (Wallace & Kelsey, 2010) in humans and E12.5 in mice, following the stimulation of the pre-GCs by inhibins to surround a single oocyte (McLaren, 1991; Chen *et al.*, 2012; Knight *et al.*,

2012). The next stage of folliculogenesis requires the transcription factor FOXL2 and the Epidermal growth factor receptor (EGFR) to facilitate the transition and recruitment of the primordial follicles to primary, secondary/pre-antral, antral and preovulatory follicles (Jamnongjit *et al.*, 2005). The transition between primordial follicles and primary follicles is marked by an increase in the cell division of GCs surrounding the oocyte. The GCs continue proliferating to form a double layer, forming two populations: the cortical or cumulus cells that immediately surround the oocyte and the mural cells that line the follicle wall (Figure 1.3). A single layer of TCs is then recruited to surround the outside of the follicle marking the transition to the secondary or pre-antral phase. Prior to the antral stage, follicle growth occurs independent of gonadotropins. The formation of the antrum, a fluid-filled cavity between the oocyte and the surrounding GCs and the differentiation of the TCs into two distinct layers, the theca interna and theca externa, marks the formation of the antral follicle. The presence of antral follicles in the ovary marks the onset of puberty and the start of follicle regulation by gonadotropins.

Prior to sexual maturity and puberty, primordial follicles located in the medulla of the ovary become activated as the first wave of follicles. They were initially believed to not contribute to fertility (Peters, 1969). In 2013, Zheng *et al.* determined that although this early wave of follicles is present primarily during non-reproductive stages, they do indeed contribute to fertility in the beginning of puberty and early sexual maturity. Since this discovery, it has been established that along with their role in fertility, it is likely that in the pre-pubertal ovary, these medullary follicles help to establish the hypothalamic-pituitary-ovarian axis, leading to the onset of puberty (Zheng *et al.* 2013).

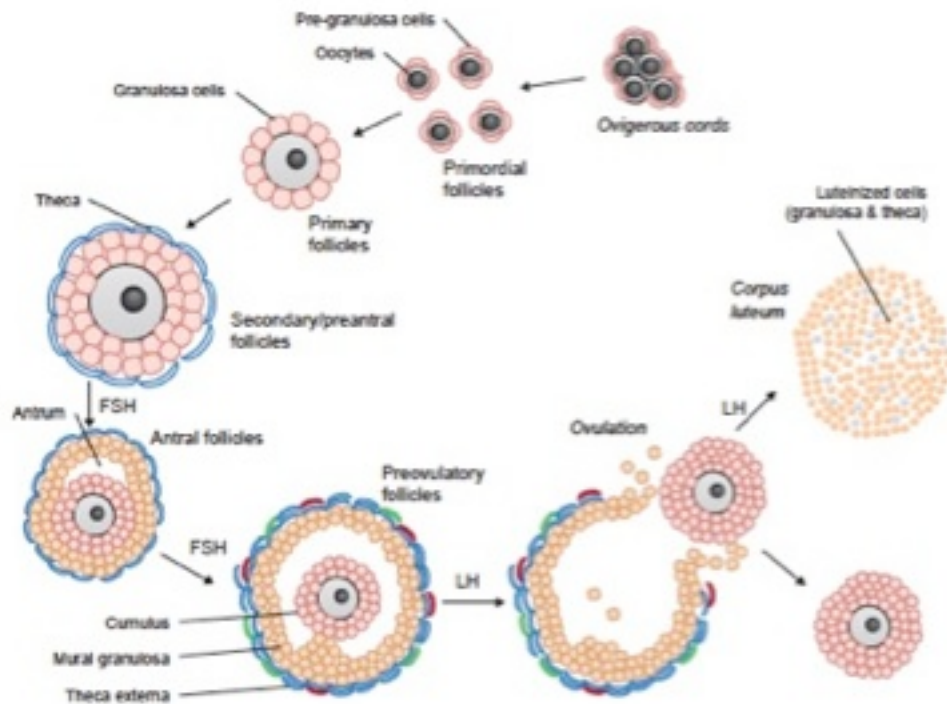


Figure 1.3 Ovarian folliculogenesis

Folliculogenesis can be separated into three main stages: primordial follicle formation, a pool of growing follicles, and lastly ovulation of the mature follicle and formation of the corpus luteum. The GCs continue proliferating to form a double layer, forming two populations: the cortical or cumulus population and the mural population. Thecal cells are then recruited to surround the outside of the follicle marking the transition to the secondary or pre-antral phase. Finally, the formation of the antrum, the theca interna and theca externa, marks the formation of the antral follicle. This is followed by ovulation of the oocyte and cumulus GC from the mature, antral follicle, which then stimulates the formation of the corpus luteum from the remaining mural GC (Used with permission from Bioscientifica Inc.).

The process of follicle recruitment has been described in two distinct follicle waves. In 1992, Hirshfield was the first to describe a heterogeneous population of primordial follicles. By observing cell proliferation, it was determined that two distinct populations of follicular cells were present; the original population in the medulla, which began to grow first, and then another population that formed at a later stage in the cortex. These findings were further supported by continuing to look at ovarian cell proliferation in rats during the embryonic period through to several weeks post delivery, where it was confirmed that indeed the pool of follicles that is present at birth, is actually a heterogeneous population with two distinct origins (Hirshfield & DeSanti 1995). This work has been expanded with the advent of new technologies to further determine the origins of the GCs and the follicles in which they are incorporated. One study that added to what was previously known looked at tracing *Foxl2*-expressing cells. In this study, it was observed that not only are there two distinct follicle populations, a medullary and a cortical, but the pre-granulosa cells of these follicles arise from different populations of surface epithelium of the ovary (Mork *et al.* 2012). It was also suggested that the first or medullary wave of follicles is anovulatory and that both waves may be unique in their morphology, development and gene expression patterns (Mork *et al.* 2012). A follow up to this study was done by Zheng *et al.* (2014) to look at these possible developmental and physiological differences between the two waves of primordial follicles. Again *Foxl2*-labeled cells were utilized as well as *Spermatogenesis and oogenesis-specific basic helix-loop-helix 1* (*Sohlh1*)-labeled cells to track each wave of follicles through fetal, adolescent and adult life. It was determined using these models that the first wave of follicles that are located in the medulla remain in the ovaries of mice from birth to

approximately 3 months where they play a role in the onset of puberty, as well as to early adulthood fertility, indicating the previous theory for their anovulatory status was not correct (Hirshfield 1992). This wave of follicles is gradually replaced by a second wave of follicles formed from a different population of surface epithelial cells and localized in the ovarian cortex. In female mice, from 3 months of age to the end of reproductive potential, this second wave acts as the primary source of ovulated follicles once the first wave has been replaced (Zheng *et al.* 2014).

1.2.2 Puberty and the establishment of reproductive cyclicity

The normal maturation process for ovarian follicles during the reproductive cycle is regulated primarily by endocrine factors, but also by paracrine signals between the oocyte, the GCs that surround the oocyte, and the TCs that surround the basement membrane of each growing follicle (Edson *et al.*, 2009; McGee & Hsueh, 2000). Steroid hormones are important for both normal ovarian function and the development of secondary sex characteristics in females. Steroid hormone production is regulated by the negative feedback loop of the hypothalamic-pituitary-gonadal (HPG) axis (Edson *et al.*, 2009; Vadakkadath *et al.*, 2005). The hypothalamus secretes Gonadotropin-Releasing Hormone (GnRH), to act on the gonadotrope cells in the anterior pituitary gland, stimulating the secretion of Luteinizing Hormone (LH) and Follicle Stimulating Hormone (FSH). Both hormones are important for both follicular development and ovulation following the start of puberty in mammals (Figure 1.4). It is after the pubertal transition that the coordinated release of LH and FSH initiate the maturation of a subset of follicles according to a species-specific estrous cycle. It is at this point in time that the TCs and GCs start to express membrane receptors for LH

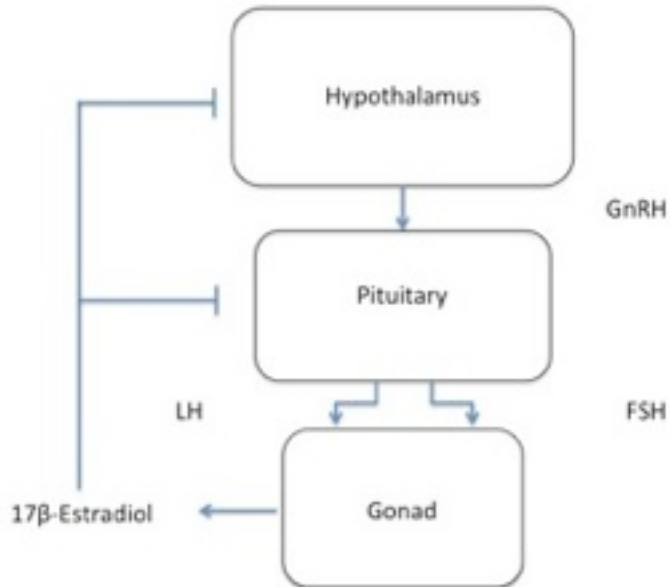


Figure 1.4 The hypothalamic-pituitary-gonadal axis

Steroid hormone production in the ovary is regulated by the hypothalamic-pituitary-gonadal (HPG) axis, which is controlled by a negative feedback loop. Gonadotropin-Releasing Hormone (GnRH) is secreted by the hypothalamus, which subsequently acts on the anterior pituitary gland to stimulate the secretion of Luteinizing Hormone (LH) and Follicle Stimulating Hormone (FSH). These hormones stimulate the release of 17β-Estradiol from the gonad, which acts to block the release of GnRH, LH and FSH from the hypothalamus and pituitary, respectively.

(LHR) and FSH (FSHR), respectively (Adashi, 1994). FSH binding to its cognate receptor promotes GCs to proliferate and express cytochrome P450, family 19, subfamily a, polypeptide 1 (CYP19A, aromatase) and 17 β -hydroxysteroid dehydrogenase (17 β -HSD), the enzymes necessary for the production of 17 β - estradiol (E₂) from androgenic metabolites produced by the TCs (Vadakkadath *et al.*, 2005). Ligand activation of the growth factor receptor EGFR acts in GCs together with FSH and LH to facilitate this normal progression of ovarian steroidogenesis (Jamnongjit, *et al.*, 2005). Upon the maturation of the antral follicles, FSH initiates their recruitment for eventual ovulation, and a surge of LH from the anterior pituitary results in the rupture of the follicle and the expulsion of the oocyte into the Fallopian tubes. To supplement its role in ovulation, FSH also prevents GC apoptosis and follicular atresia from occurring prior to ovulation. The antral follicles that have matured, but are not selected for ovulation, will die by atresia due to low FSH levels following ovulation. Post-ovulation, LH is also responsible for the luteinization of the GCs and TCs resulting in the formation of the corpus luteum, a highly vascularized tissue that produces the sex hormone progesterone (P₄; Edson *et al.*, 2009). In the absence of successful fertilization of oocyte, the secretion of E₂ and P₄ from the GCs triggers a negative feedback response in the hypothalamus to suppress the release of GnRH, while inhibins, molecules from the TGF β family, act on the anterior pituitary to suppress FSH (Knight *et al.*, 2012). As E₂ secretion declines, negative feedback inhibition is released and the follicle maturation cycle resumes according to the timelines of different species. The regulation of these gonadotropins and sex hormones is necessary for the normal development, recruitment and ovulation of follicles.

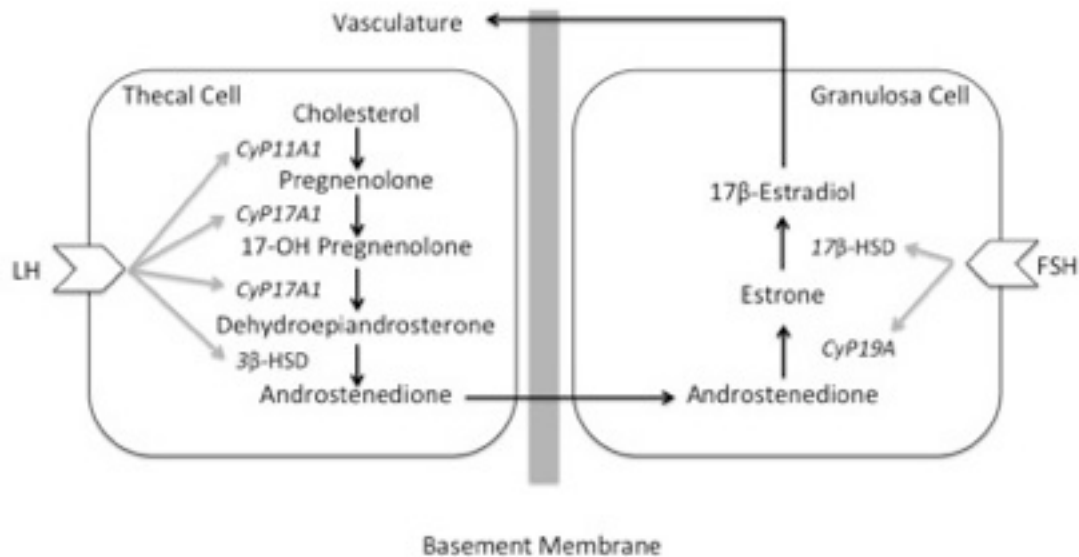


Figure 1.5 The two-cell, two-gonadotropin theory of hormone production and regulation in follicles

The normal development of follicles relies on proper paracrine function. LH stimulates the thecal cells to produce steroidogenic acute regulatory protein (StAR) to aid the transport of cholesterol. LH stimulates the thecal cells to produce three enzymes; cholesterol side-chain cleavage enzyme (CYP11A1), cytochrome P450 17A1 (CYP17A1) and 3 β -hydroxysteroid dehydrogenase (3 β -HSD). Cholesterol is converted by CYP11A1 to pregnenolone, which is then converted by CYP17A1 to first, 17-hydroxypregnenolone and then dehydroepiandrosterone (DHEA). 3 β -HSD then converts DHEA to androstenedione, which diffuses from the TCs, across the basement membrane to the GCs. The GCs then use CYP19A to convert androstenedione to estrone, which is in turn converted to E₂ by 17 β -HSD. E₂ is then released into the vasculature to provide support to follicles. [Used with permission from Kerri Smith (Masters thesis)]

The normal development of follicles relies on proper paracrine function supported by the somatic GCs and is known as the two-cell/two gonadotropin theory (Adashi, 1994). The release of FSH from the pituitary promotes not only the production of E₂ and P₄ by the GCs, but also their proliferation. LH plays a role by stimulating the thecal cells to produce steroidogenic acute regulatory protein (StAR) to aid the transport of cholesterol. LH stimulates the thecal cells to produce three enzymes; cholesterol side-chain cleavage enzyme (CYP11A1), cytochrome P450 17A1 (CYP17A1) and 3β-hydroxysteroid dehydrogenase (3β-HSD). Cholesterol is converted by CYP11A1 to pregnenolone, which is then converted by CYP17A1 to first, 17-hydroxypregnenolone and then dehydroepiandrosterone (DHEA). 3β-HSD then converts DHEA to androstenedione. This diffuses from the TCs, across the basement membrane to the GCs. The GCs then use CYP19A to convert androstenedione to estrone, which is in turn converted to E₂ by 17β-HSD (Figure 1.5; Adashi, 1994; Edson *et al.*, 2009). Over time, the release of competent, mature follicles becomes less consistent and both the endocrine and paracrine functions of the ovary begin to decline becoming less efficient as production of FSH, LH and E₂ decrease. The decrease in reproductive potential leads to the next stage of the ovarian life.

1.2.3 The post-menopausal ovary

The recruitment of follicles and ovulation is fairly constant in mammals from the onset of puberty until the pool of follicles is depleted. In humans, this timeframe of recruitment and ovulation begins with the onset of puberty and lasts for several decades after its initiation, whereas in mice it begins at 1.5-2 months of age and lasts until approximately 16 months of age (Biggers *et al.*, 1962). Once the production of hormones

necessary for normal follicle recruitment decline, so does ovulation (Finn 2001), at which time atresia of follicles increases and there is a noticeable decrease in fertility until menopause, which signals the end of reproductive potential (Gougeon, 2004).

1.3 Ovarian Tumourigenesis

In the ovary, pathologists have observed tumours arising from all potential cell types- germ cells, supporting cells and epithelial cells- suggesting the normal program and functions of these cell types confer a degree of tumourigenic risk. Tumours arising from the GC population are grouped in the sex-cord stromal tumour (SCST) class of ovarian tumours. In the human population, GC tumours (GCTs) may appear in infants, girls, young women or post-menopausal women, with broad classification as juvenile-type or adult-type tumours (Jamieson & Fuller, 2012). With the knowledge of the two distinct follicle waves, the etiology of GCTs can be explored by combining knowledge of unique GC developmental origins with molecular profiling. This is a logical strategy to subclassify tumours arising from the GC population, to improve our understanding of this ovarian tumour class and to pave the way for preventative strategies and better clinical management of the disease.

1.3.1 Granulosa cell tumours

Granulosa cell tumours are the most common subtype of SCSTs accounting for approximately 70 % of SCST cases in the human population (Colombo et al., 2007). Historically, the GCT tumour class has been divided into 2 distinct subtypes, adult and juvenile, occurring their appearance at both ends of the reproductive spectrum. The more common subtype is adult GCTs (AGCTs); these appear in older women at the end of

their reproductive life (Bjorkholm & Silfversward, 1981). At the other end of the spectrum are juvenile GCTs (JGCTs), which appear in female newborns through adolescence (Young *et al.*, 1984). The classification of the subtypes has, in the past, been based upon the age at diagnosis and tumour histology, but in recent years has moved towards using genetic and molecular characteristics to better identify the tumour subtypes.

1.3.2 AGCT of the ovary

The more common subtype of GCTs is adult (AGCTs) which occur in older women during peri- and post-menopausal phases and account for approximately 95 % of all GCTs (Bjorkholm & Silfversward, 1981). Clinically, AGCTs present with post-menopausal bleeding or secondary amenorrhea in peri-menopausal women caused by increased E₂ and inhibin α production by the tumour; however, serum E₂ levels are not indicative of disease progression as they are variable in women of different age groups (Bjorkholm & Silfversward, 1981). In a recent study of AGCTs and their biochemical properties, Kitamura *et al.* (2017) established that of 30 tumours investigated by immunohistochemistry (IHC), almost all had positive CYP19a and inhibin α expression. Elevated serum inhibin α suppresses the production of FSH from the pituitary, which partially explains the irregularity or loss of cyclic menses in peri-menopausal women with AGCT (Kitamura *et al.* 2017).

The morphology of AGCTs has allowed pathologists to describe the tumours in several different terms, including insular, macrofollicular, microfollicular, diffuse and trabecular (Lloyd, 2010). These classifications do not correspond to clinical setting and cannot be used for diagnosis and prognosis (Kitamura *et al.*, 2017). In recent years, a

recurrent, somatic, missense c.402C>G mutation in the *FOXL2* gene which results in a change to tryptophan from a highly conserved cysteine (p.C134W) residue in the FOXL2 protein was discovered by whole-transcriptome sequencing in 4 human AGCTs and subsequently confirmed in 86 AGCTs that were examined for this specific variant (Shah *et al.*, 2009; Schrader *et al.* 2009). DNA sequencing and mutation analysis results from only 4 human AGCTs was possible due to the overall genomic stability of this tumour class (Shah *et al.*, 2009). This c.402C>G mutation is heterozygous in almost all AGCTs, and unlike loss of function mutations in the *FOXL2* gene which cause BPES, the functional effect of this mutation is presumably oncogenic (Fleming *et al.*, 2010; Jamieson *et al.*, 2010). Expression of the *FOXL2* mutant gene and FOXL2 protein localization is generally unaffected in AGCTs (Schrader *et al.* 2009). This molecular finding was the first report for a consistent molecular feature in the AGCT category that has been quickly adopted as a molecular diagnostic test (Schrader *et al.* 2009).

Another important tool for the investigation of AGCTs is the KGN cell line. The KGN cell line is an immortalized, AGCT-like cell line that was developed from a tissue sample taken from an invasive, recurrent GC carcinoma of a 73-year old woman (Nishi *et al.*, 2001). After the discovery and confirmation that the somatic c.402C>G mutation in the *FOXL2* transcription factor gene was reproducibly characteristic of the AGCT subtype, the KGN cell line was investigated for the presence of the mutation. It has been reported that the c.402C>G *FOXL2* mutation is heterozygous in the KGN line by sequencing the genomic DNA (Benayoun *et al.*, 2010). For comparison to KGN, the same group investigated multiple non-ovarian and ovarian cancer cell lines of epithelial and sex cord-stromal origin, none of which harbored the mutation, supporting the specific

nature and potential diagnostic value of the *FOXL2* mutation for AGCT. The presence of the somatic *FOXL2* mutation, as well as the age of the woman from which the tissue for the cell line was obtained, has led several research groups to use the KGN line as a representative model for AGCT subtype-specific investigations (Benayoun *et al.*, 2010; Fleming *et al.*, 2010).

1.3.3 JGCT of the ovary

Juvenile GCTs (JGCTs) occur most often in newborns through adolescence, with the mean age at diagnosis being 13 yrs of age (Young *et al.*, 1984; Karalök *et al.* 2015). Clinically, patients often present with pain and distension in the abdomen, including abdominal bloating which is accompanied by premature menstruation due to their highly steroidogenic nature and the increased E₂ and inhibin α production by the tumour (Young *et al.*, 1984). When a physical examination is performed, many patients present with a palpable mass (Karalök *et al.* 2015).

The mechanism of initiation of JGCTs is unknown due in part to the rare nature of these tumours with incidence rates being only approximately 5 % of all GCTs. The occurrence of JGCTs at early time-points on the reproductive spectrum may support the hypothesis that they arise due to an underlying but unknown genetic risk factor, rather than the acquisition of somatic mutations as for AGCTs. The report by Shah *et al.* (2009) was also the first suggestion for a distinct molecular etiology for JGCTs vs. AGCTs due to the absence of the c.402C>G somatic *FOXL2* mutation in the majority of JGCTs examined (Jamieson *et al.*, 2010; Al-Agha *et al.*, 2011). Clues to the mechanism for the development of JGCTs is currently lacking.

With the FOXL2 transcription factor being intimately involved in ovarian development and GC specification, the status of FOXL2 transcript or protein expression has been an area of study for JGCT etiology. Quantitative gene expression analysis showed detectable *FOXL2* transcript in 3 JGCT samples, with expression levels at a similar order of magnitude and degree of variability as for AGCT samples (Jamieson *et al.*, 2010). IHC of JGCT tissues has also been performed to determine the FOXL2 expression status in these pediatric neoplasms. Kalfa *et al.* (2007) examined a cohort of 26 JGCT specimens for FOXL2 expression relative to normal ovary controls. This group reported reduced FOXL2 protein expression in 53 % of the JGCT cases examined (n = 14), with no FOXL2 protein expression detected in 38 % of this subset (n = 10). The authors provided a complete clinical history of the patients, leading to a significant correlation of advanced tumour staging with reduced or absent expression of FOXL2 (Kalfa *et al.*, 2007). The authors speculate that alterations of FOXL2 expression are an acquired feature in this subset of JGCTs, as the contra-lateral ovary functions normally in these patients after surgical recovery and pubertal maturation. In those JGCT specimens identified as having normal FOXL2 expression by IHC, the authors noted that FOXL2 was not abnormally sequestered in the cytoplasm (Kalfa *et al.*, 2007). Based on this limited number of studies, an examination of FOXL2 gene or protein expression in JGCT specimens has not achieved the same status as for AGTs, where the c.402C>G somatic FOXL2 mutation is considered a molecular diagnostic feature (Table 1.2). To identify molecular classifiers unique to the JGCT class, immortalized human GCT cell lines and a mouse strain that exhibits spontaneous, juvenile-onset GC tumours are models for continued exploration and discovery.

1.3.3.1 COV434 human GCT cell line

The COV434 cell line is an immortalized, human derived cell line that was isolated from a primary human GCT of a 27-year-old woman (Van Den Berg-Bakker *et al.*, 1993; Zhang *et al.*, 2000). It was initially described with 7 other ovarian cancer cell lines from serous, mucinous and endometrioid carcinomas and was determined to be a “borderline” malignant tumour by investigation of the growth characteristics and the cytogenetics, specifically trisomy on Chr 5 and structural rearrangement of Chr 22 (Van Den Berg-Bakker *et al.*, 1993). The cultured COV434 cells formed small aggregates, which were very similar to that of GCs aspirated from IVF patients indicating a cellular morphology of GCs (Zhang *et al.*, 2000). In addition to cellular morphology, one of the properties investigated was the status of *FSHR*. The COV434 cells were not found to have any mutation in the *FSHR* gene by reverse transcriptase polymerase chain reaction (RT-PCR) and the receptors were found to be intact and functioning normally (Fuller *et al.*, 1998). Another indication of GC origin is the ability to stimulate the cells with FSH to promote proliferation and secretion of E₂, suggesting the presence and proper functioning of *FSHR* in this cell line. In addition, the intercellular connections made between GCs and the cumulus oophorus were examined. It was determined that COV434 cells make intercellular connections with the cumulus oophorus, indicating the retention of some normal GC phenotypes; however, the connections are only made when an intact oocyte is present (Zhang *et al.*, 2000).

Following the detection and strong association of the p.C134W mutation in the *FOXL2* gene in AGCTs and the KGN cell line, similar investigations followed for the JGCT-like COV434 cell line. The genomic sequence of the the *FOXL2* gene in COV434

Table 1.2 Comparison of adult type and juvenile type GCTs in humans.

Characteristics	Adult-type	Juvenile-type
Frequency of GCTs in women	~ 95 %	~ 5 %
Onset	Increases risk at end of reproductive cycle	Early onset (pediatric) – infant to < 20 years
<i>FOXL2</i> status	<i>FOXL2</i> 402 C>G mutation (Shah et al. 2009)	Wildtype <i>FOXL2</i> allele
Etiology	Somatic mutation deregulates GC differentiation	Proposed germline etiology (not yet determined)

cells has been examined and it was determined that wildtype *FOXL2* is present in this cell line (Fleming *et al.*, 2010). Quantitative gene expression analyses have also been quite consistent, indicating very low expression levels of the *FOXL2* transcript in COV434 cells relative to the KGN cell line, primary JGCT samples or primary AGCT samples (Fleming *et al.*, 2010; Jamieson *et al.*, 2010; Rosario *et al.*, 2013). Although examples of *FOXL2* protein staining are not generally presented for COV434 cells in these publications, Jamieson *et al.* (2010) reported in their publication that no protein was detected by IHC methods. Much of the reported data on the COV434 cell line agrees with findings for primary JGCTs, leading to its continued use as a representative cell line for JGCTs in general, and perhaps representing a more advanced and aggressive JGCT stage based on reduced *FOXL2* expression (Kalfa *et al.*, 2007).

Since its early development (Van Den Berg-Bakker *et al.*, 1993) and subsequent characterization many years later (Zhang *et al.*, 2000), COV434 has been used by many groups as a juvenile-type GCT model, however, aside from the work done surrounding the somatic *FOXL2* mutation done after its discovery in adult-type GCTs in 2009 (Shah *et al.*, Jamieson *et al.*, 2010b; Rosario *et al.*, 2013), not much has been done to further investigate the properties which would confirm its origin. COV434 continues to be the accepted cellular model for use in exploring human GCs (Jamieson & Fuller, 2015; Pastuschek *et al.* 2015; Lunger *et al.* 2016) and will be considered as such for the purpose of this thesis and an investigation of juvenile GCT molecular properties as compared to an established mouse model early-onset GCT. Table 1.3 shows a comparison of the status of COV434 compared to the AGCT cell line KGN and the SWR mouse model.

Table 1.3 Comparison of KGN, COV434 cell lines and the SWR mouse model

Characteristics	KGN Cell Line	COV434 Cell Line	SWR Mouse Model	References
Origin	63 yr old woman (first diagnosis, sample collected at 10 yr recurrence)	27 yr old woman	Spontaneous development in mice of SWR background	Zhang <i>et al.</i> 2000 Nishi <i>et al.</i> 2001
Tumour Status	Recurrent GCT	Metastatic GC carcinoma	Primary GCT	Van Den Berg-Bakker <i>et al.</i> 1993 Beamer <i>et al.</i> 1985
FOXL2 Gene Status	Heterozygous <i>FOXL2</i> mutation	Wildtype <i>FOXL2</i> allele	Wildtype <i>Foxl2</i> allele	Fleming <i>et al.</i> 2010
	Robust <i>FOXL2</i> mRNA expression	Little to no <i>FOXL2</i> mRNA expression	No mutation in genomic DNA	Nishi <i>et al.</i> 2001 Smith <i>et al.</i> Unpublished
FOXL2 Protein Status	-	No FOXL2 expression by IHC	Normal Foxl2 expression	Rosario <i>et al.</i> 2012 Lewis <i>et al.</i> Unpublished
Classification	Adult-type GCT	“Juvenile-type” GCT	Juvenile-type GCT	-

1.3.3.2 SWR mouse model for early-onset GCT

Mice have proven to be an exceptional model for studying many human conditions due to their genetic and physiological similarities, in addition to their short gestational period. The SWR inbred mouse strain is a defined model for spontaneous, juvenile-onset GC tumourigenesis (Beamer *et al.*, 1985). This model has been described as a means to understand the genetic and endocrine triggers for early onset GC tumours (Beamer *et al.*, 1985). In SWR female mice, a restricted window for GCT initiation coincides with the pubertal transition at approximately 3 to 4 wks of age (Tennent *et al.*, 1990). Tumour-bearing females may have unilateral or bilateral masses that are macroscopically visible by 8 wks of age (Beamer *et al.*, 1985; Tennent *et al.*, 1990). If no GC tumours develop within this period, the mouse will remain unaffected and fertility will be normal over the course of the reproductive lifespan. (Figure 1.6, Figure 1.7)

The GCTs that arise in SWR female mice are hormone-dependent, with a requirement for the endocrine environment of puberty to trigger tumour initiation. The importance of steroids and the HPG axis has been demonstrated by the implantation of genetically susceptible, pre-pubertal SWR ovaries into immunocompromised mice with no sex steroid production (*scid/scid; hpg/hpg*), to avoid graft rejection and test the influence of the endocrine environment on GC tumour initiation. The outcome was complete suppression of GCT initiation in an environment devoid of gonadotropins and sex steroids, suggesting that an intact HPG axis is necessary for tumour formation (Beamer *et al.*, 1993). By treating the *scid/scid;hpg/hpg* recipient with human chorionic gonadotropin (hCG) to mimic the effects of LH, or with direct androgenic metabolites such as DHEA and testosterone, GC tumour initiation was rescued, indicating the

importance of androgenic stimulation to GC tumourigenesis in this model (Beamer *et al.*, 1988a; Tennent *et al.*, 1993; Dorward *et al.*, 2007).

In SWR female mice, the trait of GCT susceptibility is heritable but trait penetrance is incomplete, ranging from < 1 % to > 25 %, depending on the endocrine environment and the genetic background (Beamer *et al.*, 1985). For example, treatment of pubertal SWR female mice with exogenous androgens through diet supplementation or implants (slow release subcutaneous capsules) both act to increase tumour penetrance from <1 % to \geq 25 % (Beamer *et al.*, 1988b). Another strategy to overcome low trait penetrance without manipulation of the steroid environment came to be realized through mapping crosses designed to identify the genes responsible for GC tumour susceptibility. At least 3 discrete *Granulosa cell tumour (Gct)* susceptibility loci have been mapped to high resolution in the SWR strain: *Gct1* located on Chr 4 (Beamer *et al.*, 1988b; Beamer *et al.*, 1998a; Dorward *et al.*, 2005; Dorward *et al.*, 2013; Smith *et al.*, 2013) and *Gct4* and *Gct6* located on Chr X (Beamer *et al.*, 1998b; Dorward *et al.*, 2003; Dorward *et al.*, 2013). *Gct1* has been resolved to 1.65 mega bases (Mb; Beamer *et al.*, 1988b; Dorward *et al.*, 2013; Smith *et al.*, 2013). This locus has been reported by mapping to be fundamental for tumour initiation with SWR contributing the susceptibility alleles (*Gct1^{SW}*). *Gct1^{SW}* behaves like an oncogene, since one copy is sufficient to confer GC tumour susceptibility, but two copies render GCT initiation more probable, but with the same pubertal timing (Beamer *et al.*, 1988a). *Gct4* and *Gct6* are discrete loci on Chr X, over 35 Mb apart in the equivalent segment of the long arm of human Chr X (Xq); (Dorward *et al.*, 2003). The *Gct6* locus was mapped as a GC tumour suppressor allele, although the definitive identity of the *Gct6* gene is yet to be determined (Dorward *et al.*, 2003;

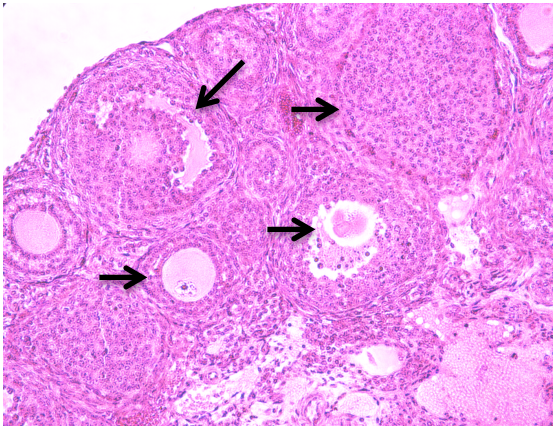
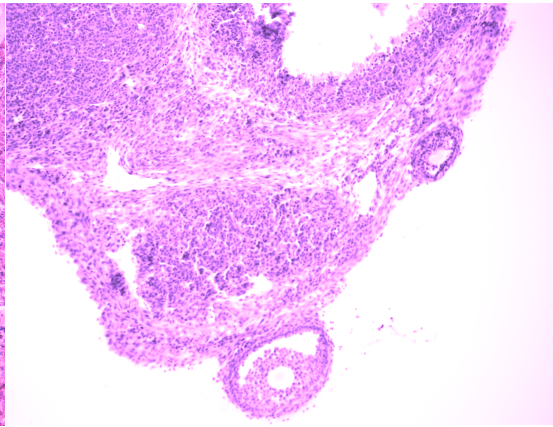
A**B**

Figure 1.6 Histology of normal whole ovaries (A) and granulosa cell tumours (B) from SWR mice

Normal whole, ovaries and sections of GCTs from SWR mice were fixed, stained with Hematoxylin and Eosin (H & E) and imaged at 20X. In A, you can see the follicles and normal cellular organization of the ovary. Arrows represent follicles in different stages and the GCs surrounding the oocyte. In B, the homogeneous cellular makeup of the GCTs can be observed with remnants of ovarian follicles forced to outer regions.

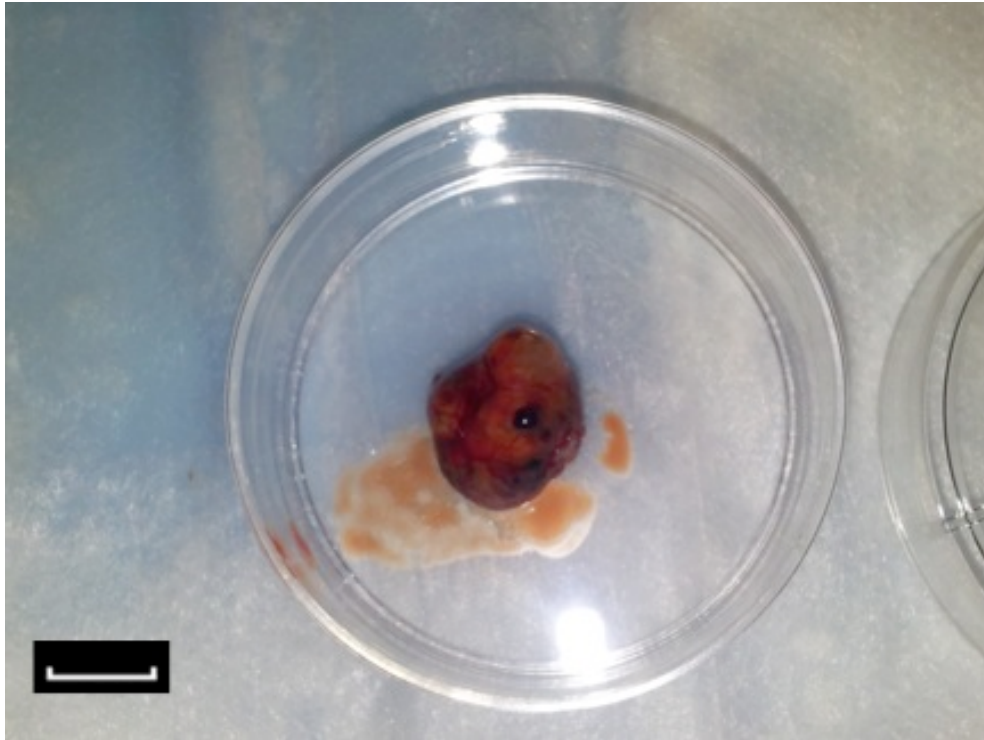


Figure 1.7 Gross GCT specimen from SWR mouse.

A GCT extracted from a SWR background mouse. This tumour was a unilateral solid mass with cystic masses and blood filled spaces. Culture dish is 5 cm. (Scale bar = 1 cm)

Dorward *et al.*, 2013). The *Gct4* locus is reported to be a strong modifier of GC tumour susceptibility; a likely candidate for the identity of *Gct4* is the Androgen receptor gene (*Ar*) due to the role of androgens in GCT initiation and its location within the *Gct4* loci (Dorward *et al.*, 2003). The homozygous congenic strain, SWR.CAST-X₁, harbours a unique *Gct4* locus to render females more susceptible to spontaneous GC tumour development (~ 20 %) without endocrine manipulation by diet or surgical implants (Dorward *et al.*, 2013). Similar GC tumour penetrance is also observed in F1 generation daughters obtained by crossing SWR dams and SWR.CAST-X₁ sires, due to a strong paternal effect at *Gct4* (Dorward *et al.*, 2013). Developing a higher penetrance model allows investigation of multiple spontaneous GCTs where the biology of tumour initiation can be examined without the influence of external hormones. Interestingly, the mapped *Gct* loci did not implicate variation in the *Foxl2* gene as a heritable susceptibility factor. An investigation of the *Foxl2* gene sequence in SWR strain genomic DNA and cDNA generated from GCTS verified the expected reference genomic sequence with no evidence of somatic mutation in *Foxl2* cDNA collected from GCTs (Smith *et al.*, unpublished). Likewise, it has been noted that BPES patients with heritable mutations in *FOXL2* do not exhibit increased susceptibility to GC tumorigenesis, suggesting other loci have greater influence (Kalfa *et al.*, 2007).

Many properties of the SWR mouse GCT model are similar to the JGCT class of human tumours. For example, established GCTs of SWR female mice are highly steroidogenic, producing high levels of both E₂ and inhibins similar to human GCTs (Beamer *et al.*, 1988a). In addition to increased production of E₂, the mouse tumours also

result in decreased production of GnRH, FSH and LH by the HPG axis, as well as lower than normal levels of P₄, T and dihydrotestosterone (DHT) in serum (Beamer, 1986). This is due to a normal suppression of the HPG axis by the increased E₂ production (Figure 1.3). The early window of GCT initiation in SWR female mice also shows similarities with pediatric JGCT onset and points to the development of the tumours from the first wave of ovarian follicles (Zheng *et al.* 2014). The overall parallels with the human JGCT condition make this model appropriate for investigating pathways of JGCT tumourigenesis and its potential genetic contributions.

1.4 Experimental Rationale

As an experimental model of juvenile-onset GC tumourigenesis, the SWR inbred mouse strain provides a unique opportunity to investigate the genetics, endocrinology and tumour biology of JGCTs. The focus of this thesis investigation is the protein expression profile of normal mouse ovaries collected from the SWR.CAST-X₁ congenic strain, vs. genetically-matched, spontaneous GCTs collected at 6-8 wks of age following tumour initiation at puberty. Included in the protein profile are transcription factors, enzymes, and receptors known to be expressed in the GC populations (Egfr, Esr2, Cyp19a, Fshr) and proteins known to play a role in gonad specification, transdifferentiation and/or GC tumourigenesis (Foxl2, Sox9). In addition to a comparison of the normal ovaries vs. overt GC tumours, protein lysates collected from the COV434 JGCT-like cell line will be compared to the mouse GCTs, to identify any common features, in the search for a biomarker of JGCT identity.

1.5 Hypothesis and Research Objectives

1.5.1 Hypotheses:

1. Juvenile-onset GCT specimens collected from SWR female mice < 8 wks of age are proliferative, benign tumours that will retain the expression profile of age-matched normal ovaries for proteins of importance to ovarian physiology: Egfr, Fshr, Cyp19a and Esr2.
2. GCT initiation in female SWR mice is an abnormal response to the normal endocrine stimulation of puberty, involving changes in the protein expression profile of the gonad specification factors Foxl2 and Sox9.
3. Juvenile-onset GCT specimens collected from SWR female mice will have similar protein expression profiles to the COV434 cell line that is classified as a human JGCT model.

1.5.2 Research Objectives

- 1) Using an immunoblotting technique, I will compare protein expression profiles for 6 fertility or gonad-specification proteins between normal ovaries and spontaneous, primary GC tumour samples collected from age-matched SWR-derived congenic female mice.
- 2) Using an immunoblotting technique, I will compare protein expression profiles for 6 fertility or gonad-specification proteins between spontaneous, primary GC tumour samples collected from SWR-derived congenic female mice and the COV434 juvenile-type GC tumour cell line.

2.0 Materials and Methods

2.1 Animal Husbandry and Protocol Approvals

Mice were housed in the central animal care facility of the Health Sciences Centre at Memorial University of Newfoundland. The Institutional Animal Care Committee, in accordance with Canadian Council on Animal Care guidelines, approved all animal care protocols (14-01-AD, 14-04-AD). Mice were given Laboratory (autoclavable) Rodent Diet 5010 chow (27.5% protein, 13.5% fat, 59% carbohydrate; LabDiet Co., St.Louis, MO) with sterile water *ad libitum*, and were housed under a 12:12 hour (h) light/dark cycle. Mice were weaned at 20-23 days (d) of age and housed in groups of 2 to 5 animals per 27.94 cm (L) x 17.78 cm (W) x 12.7 cm (Ht) rodent cages in an individually ventilated caging system (Tecniplast, West Chester, PA) containing Bed-O-Cobs® corn-cob bedding material (The Andersons, Maumee, OH) with additional housing and bedding enrichment.

2.2 Tissue Sample Collection

Homozygous female mice of the SWR-derived congenic strain SWR.CAST-X₁, or F1 female offspring from (SWR x SWR.CAST-X₁) breeding pairs were used in this experiment given their heritable tendency for spontaneous GCT initiation at puberty (Tennent, Shultz, Sundberg, & Beamer, 1990). Female mice were euthanized by exposure to carbon dioxide (CO₂) gas at 6 - 8 wks of age for inspection of the peritoneal cavity and the presence of unilateral or bilateral GCTs. Normal, whole ovaries were extracted and pooled from a single female for protein lysate preparation. When a unilateral or bilateral GCT was observed, the tumour was extracted and pieces of the tumour cleaned from as much blood as possible in a dish of sterile saline (0.85 % NaCl). GCT tissue fragments of

approximately 5-7 mm³ were processed for protein lysate preparation. Male mice of the SWR/Bm and C57B6 backgrounds were also harvested to extract prostate and testis tissue for immunoblotting and immunohistochemical analysis as control tissues for the Sox9 protein. To facilitate labeling, all tissue sample lysates were identified with a labeling system that used a letter for tissue type and a unique number for independent specimens. For example, N1 represents the sample collected for normal, pooled ovaries from a single unaffected female, whereas T1 represents a tumour fragment from a unilateral tumour from a single affected female, or T1A and T1B for individual fragments from bilateral tumours from a single affected female. Prostate tissue was labeled P1.

The protein lysates for normal ovaries, GCT tissue samples and prostate were prepared in Radioimmunoprecipitation assay (RIPA) lysis buffer comprised of: deionized water, 1 x Protease Inhibitor Solution (Roche, Mississauga ON), 0.05 M Tris-Hydrochloric Acid (HCl) pH 7.4 (Life Technologies, Carlsbad, CA), 0.005 M ethylenediaminetetraacetic acid (EDTA), 0.05 M Sodium Fluoride (VWR International, Radnor, PA), 1 x Dulbecco's Phosphate Buffered Saline (PBS; Life Technologies, Carlsbad, CA), 0.1 % Sodium Dodecyl Sulfate (SDS; ThermoFisher Scientific, Waltham, MA), 1 % TritonX 100, 0.5 % Deoxycholate, 0.05 M β - Glycerophosphate, 0.001 M Sodium Orthovanadate, and 0.125 ng/mL phenylmethanesulfonyl fluoride (PMSF) all purchased from Sigma-Aldrich, St. Louis, MO unless otherwise stated. A pair of normal ovaries (< 1 g) was lysed in 50 μ l of RIPA buffer, while GCT fragments and prostate (~ 1 g) were lysed in 100 μ l. Samples were homogenized in buffer using a Pellet Pestles Cordless Motor (Sigma-Aldrich, St. Louis, MO) and Kontes ® Pellet Pestle ® Grinders

(Kimble Chase, Vineland, NJ). Once the tissue was homogenized, the pestle was rinsed with 50 or 100 μ l of RIPA lysis buffer (depending on the amount of tissue).

Both homogenate and rinse were combined to compose the final tissue sample lysate. The sample lysates were centrifuged for 10 min at a speed of 21,000 x g at 4 °C (Thermo IEC Micromax Centrifuge) and the supernatant transferred to a fresh 1.5 mL microcentrifuge tube that was then stored at -80 °C until the time of protein assay.

2.3 COV434 Cell Culture

COV434 cells were cultured as monolayers on cell culture plates (Greiner Bio-One, Monroe NC) with DMEM plus 2 mM glutamine (Life Technologies, Carlsbad, CA), and supplemented additionally with 10 % Fetal Bovine Serum (FBS; ThermoFisher Scientific, Waltham, MA). The plates were incubated under standard culture conditions (37 °C, 5 % CO₂; Forma™ Series II Water Jacket CO₂ Incubator, ThermoFisher Scientific, Waltham, MA). Cells were passaged when they reached an estimated confluence of 80 % into new cell culture plates by washing cells 3 times with PBS before adding 1 mL of 0.25 % Trypsin-EDTA to detach the cells from the plate. The plate was incubated for 1-2 min to allow cells to detach before resuspending cells in DMEM media and distributing into new cell culture plates at a 1/3 dilution.

2.4 COV434 Sample Collection

COV434 cells were plated in 6 well culture dishes at 1/3 density and grown to 80 % confluence before protein lysate extraction from approximately 600,000 cells directly in the culture plate. The culture plates were placed on ice, the medium was aspirated and cells were washed 3 times per well with cold PBS (ThermoFisher Scientific, Waltham, MA). After washing, ice-cold RIPA lysis buffer (60 μ l per 34.8 mm diameter well) was

added and the plate was tilted to fully cover the adherent cells. The plate was left on ice for 5 min after which it was tilted and left for an additional 5 min on ice. Each monolayer slurry was then scraped using a cell scraper (Corning, Corning, NY), combining the contents of 3 wells per 6-well plate into one 1.5 mL microcentrifuge tube as an independent COV434 sample. The tube was spun at 4 °C for 10 min at 21,000 x g (Thermo IEC Micromax Centrifuge) and the supernatant, approximately 180 µl, transferred to a fresh, labeled 1.5 mL microcentrifuge tube for storage at -80 °C until the time of protein assay. Using a similar labeling strategy as for normal ovaries and GCT samples, independently collected COV434 lysates were identified as C1, C2, C3, etc.

2.5 Tissue Fixation

2.5.1 Hematoxylin and Eosin Staining & Brightfield Imaging

GCT tissue or normal ovaries collected at necropsy from genetically susceptible female mice were fixed in 4 % paraformaldehyde-PBS (pH 7.4) at room temperature overnight on a rotator and transferred to 70 % ethanol (EtOH) for Hematoxylin and Eosin (H&E) staining prior to paraffin embedding at the central Medical Education and Laboratory Support Services department (MELSS; Health Sciences Centre, Faculty of Medicine). After embedding, the tissues were sectioned at a thickness of 5 µm and mounted on glass slides for photomicroscopy.

2.5.2 Tissue collection for immunohistochemistry (IHC)

GCT tissue and normal ovaries from SWR strain background mice that were treated with DHEA capsules at 3 wks of age to induce tumour formation, were isolated and collected at necropsy at 8 wks of age (Smith *et al.* 2013) from litter matched

genetically susceptible female mice and fixed in Bouin's solution at room temperature for 24 h on a rotator. Testis control tissue from wildtype male mice of the C57BL/6J background were isolated and collected at necropsy at 3.5 wks of age and fixed in Bouin's solution at room temperature for 4 h on a rotator, Fixation occurred prior to paraffin embedding at the central MELSS (Health Sciences Centre, Faculty of Medicine). After embedding, the tissues were sectioned at a thickness of 5 μ m and mounted on glass slides for IHC analysis (see section 2.10).

2.6 Brightfield Imaging

H&E stained sections were imaged using a Leica DM-IRE2 inverted microscope (Leica Microsystems, Richmond Hill, ON) attached to a Retiga Exi CCD camera (QImaging, Burnaby, B.C.). Image capture was done using Openlab Image Analysis software (Version 5.5; Improvision, Inc., Lexington, MA) to observe the histology of normal SWR mouse ovaries and primary GCTs. SWR normal ovaries and primary GCTs were viewed and imaged at a magnification of 20 x and 40 x. Image contrast and brightness were adjusted uniformly to the images using Adobe Photoshop (San Jose, CA).

2.7 BCA Protein Assay

Protein lysates were assayed using a BCA Protein Assay (ThermoFisher Scientific, Waltham, MA) to determine the protein concentration of each sample. Using 1 mg/mL bovine serum albumin (BSA; ThermoFisher Scientific, Waltham, MA) as a stock protein standard, a 96 well plate (VWR International, Radnor, PA) was loaded in duplicate wells with a protein concentration gradient of 0, 2.5, 5, 10 and 20 μ g BSA combined with 2 μ l RIPA lysis buffer per well. Similarly, 2 μ l of the experimental

samples were loaded into duplicate wells and the corresponding lysis buffer sample was loaded into separate wells, in duplicate, as a blank. Pierce™ BCA kit reagents (ThermoFisher Scientific, Waltham, MA) A and B were mixed at a 50:1 ratio, respectively to have sufficient volume to add 300 µl of the solution to each standard and experimental sample well. The plate was incubated at 37 °C for 30 min and read on a POLARStar OPTIMA Plate Reader (BMG LABTECH Inc., Cary, NC) at an absorbance of 562 nm. The optical density was compared against the standard protein concentration and a linear regression line was used to determine the amount of protein in unknown samples. The sample absorbance values were used to calculate the total protein concentration (µg/µl) of each sample. The concentration of protein (µg/ µl) was utilized to calculate the amount of sample (µl) that was required to obtain the desired protein amount (µg) for immunoblotting (10, 20 or 30 µg).

2.8 Immunoblotting

a. Electrophoretic separation of proteins

Protein lysates made from normal ovary pairs, primary GCTs and the human COV434 cell line, were used to investigate the expression profile of 6 proteins; Cyp19a, Egfr, Esr2, Foxl2, Fshr, and Sox9. Once the desired volume of protein lysate was identified to achieve 10, 20 or 30 µg of total protein, it was added to 5X Sample Buffer [5 x Sample Buffer Solution; 10 % glycerol, 5 % SDS, 50 mM TRIS-HCl pH 7.5 (ThermoFisher Scientific, Waltham, MA) and 0.125 % bromophenol blue (VWR International, Radnor, PA) and 5 % β-mercaptoethanol (BME, ThermoFisher Scientific, Waltham, MA)]. To denature the protein, the samples were heated to 100 °C for 4 mins and centrifuged for 10 sec before loading. Acrylamide separation gel percentage was

determined based on the molecular weight of the particular protein of interest; proteins larger than 80 kDa, as predicted by the antibody product sheet, were separated on a 7.5 % gel, while proteins smaller than 80 kDa were separated on an 8.5 % gel. The molecular weight and percent gel for each protein of interest are listed in Table 2.1. Gel composition was made up as per Roberts *et al.* (1984).

PageRuler Plus Protein Ladder (Invitrogen, Carlsbad CA) was loaded into the first well and all samples were loaded slowly to prevent mixing using gel loading tips (ThermoFisher Scientific, Waltham, MA). A prestained protein ladder was used to visualize the approximate size of the proteins of interest. By knowing the approximate size of each protein, we were able to match each band to the matching stained band of the appropriate size. All sample types - N, T and C - were analyzed together on a single blot with a particular antibody. Multiple blots of the same samples were analyzed to account for variability between immunoblotting assays. The gel was run at 15 mA until samples had completely passed through the stacking gel, after which they were run at 22 mA for approximately 1 h to achieve size separation. A Mini-PROTEAN Tetra Cell system (Bio-Rad, Hercules, CA) was used for all protein electrophoresis.

b. Protein transfer to a solid support membrane

All proteins separated by electrophoresis were transferred to Polyvinylidene fluoride (PVDF) membrane (Millipore, Billerica, MA). The transfer sandwich was assembled as per manufacturer's instructions (Bio-Rad, Hercules, CA). Protein transfer was performed at 100 V for 45 min in transfer buffer [25 mM TRIS base, 192 mM Glycine, 20 % Methanol (VWR International, Radnor, PA) chilled to 4 °C. Upon transfer

completion, the membranes were trimmed to the size of the gel, nicking the bottom right hand corner to maintain the correct orientation. The gel was checked for transfer efficiency by looking for the presence of bands from the pre-stained ladder standard on the gel prior to discarding to determine whether total protein transfer was accomplished.

c. Immunoblotting

After transfer, the PVDF membranes were quickly rinsed and placed in 10 mL of a blocking solution containing 5 % non-fat skim milk in TRIS buffered saline with Tween-20 [TBST; 0.01 M TRIS-HCl pH 7.4 (ThermoFisher Scientific, Waltham, MA and Invitrogen, Carlsbad, CA), 0.14 M NaCl and 0.1 % Tween-20 (VWR International, Radnor, PA)]. The blots were placed on a rocking platform at room temperature for at least 45 min. While the membranes were blocking, primary antibody dilutions were prepared. All primary antibodies were diluted in 6 mL of blocking solution. Working dilutions for each antibody are listed in Table 2.1. After blocking, the solution was discarded and the membranes were placed in primary antibody to incubate on the rocking platform at 4 °C overnight.

The membranes were then washed 5 times for 5 min each in TBST (approximately 10 mL per wash) on a rocking platform at room temperature. Following washing, the membranes were incubated with secondary antibody (Table 2.1) conjugated to horseradish peroxidase (HRP; Santa Cruz, Santa Cruz, CA) at a 1:5000 dilution in blocking solution for 1.5 hrs rocking at room temperature. After secondary antibody incubation, the membranes were transferred to clean containers and washed again in TBST, 5 times for 5 min. After washes, the membranes were placed in SuperSignal®

Table 2.1 Detailed list of antibodies used in immunoblotting and IHC.

Antibody Target Protein	Clone #	Company	Molecular Weight (kDa)	Gel Percentage (%)	Primary Antibody Dilution	Secondary Antibody	Secondary Antibody Dilution
Cyp19a	H-300	SCB	50-58	8.5	1:500	Goat anti-rabbit IgG-HRP	(1:5000)
Egfr	1005	SCB	170	7.5	1:500	Goat anti-rabbit IgG-HRP	(1:5000)
Esr2	H-150	TFS	55	8.5	1:500	Goat anti-rabbit IgG-HRP	(1:5000)
Foxl2	H-43	SCB	38	7.5	1:500	Goat anti-rabbit IgG-HRP	(1:5000)
Fshr	H-190	SCB	75	8.5	1:500	Goat anti-rabbit IgG-HRP	(1:5000)
Sox9	H-90	SCB	65	8.5	1:500	Goat anti-rabbit IgG-HRP	(1:5000)
Sox9	82630	CST	70	8.5	1:1000 (immunoblotting) 1:400 (IHC)	Goat anti-rabbit IgG-HRP	(1:4000)
β - actin	3700	CST	45	7.5	1:10000	Goat anti-mouse IgG-HRP	(1:15000)
α/β - Tubulin	2148	CST	55	7.5 or 8.5	1:1000	Goat anti-rabbit IgG-HRP	(1:5000)

* SCB- Santa Cruz Biotechnology, TFS- ThermoFisher Scientific, CST- Cell Signaling Technology

* Molecular weights listed are expected weights as per antibody product sheet.

West Pico Chemiluminescent Substrate (ThermoFisher Scientific, Waltham, MA) with the A and B reagents mixed in a 1:1 ratio and incubated, with shaking, at room temperature for 5 min. The membranes were removed from the substrate, allowing any excess to drain, placed on a plastic backing, covered in plastic wrap (Kirkland Signature, Kirkland, WA), and placed in a x-ray cassette. In a dark room, protein bands were visualized by exposing CLINICSELECT Green X-ray film (Carestream Health, Rochester, NY) or Amersham Hyperfilm™ ECL film (GE Healthcare, Pittsburgh, PA) and developed (Mini Med Film Processor, AFP Imaging Corporation, Elmsford NY).

The membranes were stripped to enable re-probing with an antibody to a housekeeping cellular protein as a loading control. Membranes were stripped (distilled water, 1% SDS, 20 mM TRIS-HCl pH 6.8 and 0.8 % BME) for 10 min in a shaking water bath at 50 °C. After incubation, the membranes were washed twice for 5 min each in TBST. The membranes were blocked and washed as previously described. Tubulin- α/β (Cell Signaling Technology, Danvers, MA) was used as a loading control for all proteins with the exception of Egfr, for which we used β -actin (Cell Signaling Technology, Danvers, MA) as a loading control. All tubulin or β -actin antibodies were diluted in blocking buffer and are listed in Table 2.1. The same procedure was followed for the loading control proteins, as with the proteins of interest, with the exception of using a mouse HRP-conjugated secondary antibody (Santa Cruz, Santa Cruz, CA) for β -actin. To account for variability between immunoblotting assays, all sample types, normal, whole ovary, GCT and COV434 lysates, were analyzed together on a single blot, allowing for multiple biological replicates to be analyzed relative to each other. For Cyp19a, Egfr, Esr1 and Sox9, a total of 6 biological replicates were analyzed. For Foxl2 and Fshr, 5

biological replicates were analyzed. Biological replicates were repeated 2 or 3 times to minimize technical variability between identical samples (Appendix B). An additional replicate of the Sox9 protein was completed using a monoclonal Sox9 antibody (Cell Signaling Technology, Danvers MA) to confirm prior immunoblotting results. Films were scanned in black and white at 600 dpi using a Canon MX450 series scanner. Saturation of the bands was determined by visual inspection, which is a limitation of this technique. Images were saved as JPEG files and analyzed in ImageJ 1.47v (<http://imagej.nih.gov>, National Health Institute) to obtain pixel density of each protein band.

2.10 Immunohistochemistry

Bouin's fixed tissues were embedded in paraffin, sectioned at a 5 µm thickness and mounted on VWR® Superfrost® Plus Micro Slides (VWR International, Radnor PA) at the central Medical Education and Laboratory Support Services (MELSS) department (Health Sciences Centre, Faculty of Medicine). Slides were held in a 45 °C drying oven overnight to ensure section adherence before processing. Normal female mouse ovaries, male mouse testes and mouse GCT samples were included in the immunohistochemistry (IHC) analysis.

To start, tissues adherent to glass slides were deparaffinized and hydrated by a manual processing strategy, as follows; xylene tanks (3 x 5 min) followed by 100 % ethanol tanks (2 x 10 min), 95 % ethanol tanks (2 x 10 min) and lastly into ddH₂O (2 x 5 min) each. After deparaffinization, 15 mL of concentrated Citrate buffer (Vector Laboratories, Burlingame CA) was added to 1.6 L of ddH₂O in a pressure cooker to start antigen retrieval (Deni® model). The slides were immersed in diluted Citrate Buffer

solution (pH 6.0) and pressurized at the high temperature setting for 5 mins. After the cooker depressurized slowly, the slides were removed and washed in ddH₂O (2 x 5 min).

The slides were subsequently placed in 3 % hydrogen peroxide (H₂O₂) for 10 min to quench the endogenous peroxidase activity, followed immediately by ddH₂O twice for (2 x 5 min) and 1X TBST (1 x 5 min). The blocking serum was prepared by adding 6 drops of stock goat anti-rabbit serum from the VECTASTAIN Elite ABC Reagent Kit (Vector Laboratories, Burlingame CA) to 20 mL of 1X TBST. Each slide was blotted with filter paper to remove excess TBST and tissue samples were outlined using an ImmEdgePen (Vector Laboratories, Burlingame CA) to Immunoglobulin G (IgG) control and primary antibody-treated sections. After tissue sections were isolated with a hydrophobic perimeter, slides were placed horizontally in a hydration container and spotted with blocking serum at room temperature for 60 min. During the blocking serum incubation, the primary antibodies were prepared on ice. A rabbit-derived monoclonal antibody for Sox9 protein (Cell Signaling Technology, Danvers MA), was prepared at a 1:400 dilution in blocking serum with a respective rabbit IgG (negative control; Santa Cruz, Santa Cruz CA), prepared at an equivalent dilution in blocking serum to that of the Sox9 antibody. After 60 min of blocking, the slides were blotted to remove excess blocking serum and the slides were placed back into the hydration container. Tissues were immediately spotted with their respective IgG control and or Sox9 primary antibodies. Antibody incubations proceeded overnight at 4 °C.

The following day, the secondary biotinylated antibody reagent was prepared by adding 1 drop of the biotinylated antibody stock from the VECTASTAIN Elite ABC Reagent Kit to 10 mL freshly prepared blocking serum in TBST (3 drops per 10 mLs).

The ABC detection reagent was prepared in a separate tube by adding 2 drops of Reagent A to 5 mL of 1X TBST, inverting to mix and then adding 2 drops of Reagent B followed by mixing. The ABC Reagent solution was prepared at least 30 min prior to slide application, as recommended by the manufacturer's instructions.

Slides were blotted to remove the primary antibody and washed in tanks of fresh 1X TBST (3 x 5 min). The slides were placed back into the hydration container and coated with the secondary antibody and left to incubate for 30 min at room temperature. Following the incubation, each slide was blotted and placed into fresh 1X TBST (3 x 5 min). The slides were placed back into the hydration container and coated with the prepared ABC Reagent and incubated for 30 min at room temperature. During this incubation, the 3,3'-diaminobenzidine (DAB) Substrate was prepared by adding 2 drops of the DAB Chromogen concentrate to 2 mL of ImmPACT DAB Diluent and vortexing to mix (ImmPACT DAB; VECTASTAIN Elite ABC Reagent Kit, Vector Laboratories, Burlingame CA). This solution was protected from light to prevent activation prior to application.

Following 30 min in the ABC reagent, the slides were blotted before placing them into fresh 1X TBST for 5 min and then dipping them quickly in ddH₂O (5 dips). Slides were blotted once more, placed into the hydration container and the tissue sections spotted with DAB substrate. Slides were incubated with the DAB substrate for up to 25 min or until colour was evident in the positive control testis tissues for Sox9 staining. Slides were blotted and placed in ddH₂O for 5 min to remove excess DAB substrate. The tissues were then dehydrated by dipping the slides 20 times each in 95 % ethanol (x2 tanks), 100 % ethanol (x2 tanks) and xylene (x2 tanks). Coverslips were added to each

slide using VectaMount Mounting Medium (Vector Laboratories, Burlingame CA), carefully so as not to introduce any air bubbles and the slides were cleaned with xylene soaked gauze. Slides were laid flat to dry and stored at 4 ° C prior to brightfield imaging and digital image capture.

2.11 Statistics

Microsoft Excel (Microsoft, Redmond WA) was used to calculate the densitometric relative amount of proteins of interest to its respective loading control from the same transfer membrane. Once the ratios were determined, these normalized values were entered in GraphPad Prism (GraphPad Software, Inc., La Jolla CA) to perform one-way ANOVA with Tukey's Multiple Comparison Test to determine differences in the expression pattern between normal, mouse GCT or the human COV434 cell lysates. For this purpose, a p-value ≤ 0.05 was considered significant.

3.0 Results

GCTs appear in SWR-derived female mice with a tumour frequency of approximately 20 % in high penetrance crosses. In this study, a total of 288 females were examined from (SWR x SWR.CAST-X₁) F1 generation matings at age 6 wks, with 32 GCTs macroscopically identified (11.1 % frequency). GCTs for protein lysates were selected based on the presence of viable tissue (non-necrotic) and sufficient tissue availability after microdissection and rinsing away excess blood, in order to collect 6 individual spontaneous GCTs for protein lysates (Appendix B). Although GCTs isolated from young SWR female mice and the COV434 cell line possess similar presentation features that support their exploration as JGCT model systems, this is the first time they have been directly compared for protein expression. A complement of six proteins influential for gonadal development and ovarian function - Cyp19a, Egfr, Esr1, Foxl2, Fshr and Sox9 – were examined by immunoblotting in normal, whole ovaries and spontaneous GCTs isolated from SWR-derived female mice, as well as the human JGCT-like cell line COV434.

3.1 Immunoblotting Analysis

Cyp19a

The expression of Cyp19a enzyme was examined in normal whole mouse ovaries, age-matched mouse GCT specimens and COV434 whole cell lysates by immunoblotting, using a polyclonal antibody suited for cross-species protein detection. A representative immunoblot exhibits a 58 kDa relative molecular weight (M_r) band for Cyp19a in all experimental samples, relative to an α/β Tubulin loading control (55 kDa) that was used

to normalize the expression for each individually loaded sample (Figure 3.1). A quantitative comparison of the normalized mean band density revealed no significant difference in the expression of Cyp19a between normal whole ovaries or GCTs or between normal whole ovaries or the COV434 cell line; however, the mean level of Cyp19a expression was approximately 4-fold higher in the COV434 cell line compared to GCTs having statistical significance with a p-value of 0.0254 (n= 6 per group).

Fshr

Likewise, the expression of the gonadotropin receptor Fshr was examined between normal whole mouse ovaries collected from the SWR-derived female mice, independent mouse GCT specimens and COV434 whole cell lysates by immunoblotting, using a polyclonal antibody suited for cross-species protein detection. A representative immunoblot exhibits Fshr detection at a M_r of 76 kDa in all samples examined, using the loading control band for α/β Tubulin to normalize the expression for each individual sample (Figure 3.2). No significant differences in the expression of Fshr were found between the normalized band density of the three experimental groups (n = 5 per group), however there appeared to be slightly higher expression in the normal ovarian samples.

Egfr

Egfr expression was examined in normal whole mouse ovaries, mouse GCT specimens and COV434 cell lysates by immunoblotting using a polyclonal antibody that has cross-species reactivity. The Egfr banding pattern exhibited a M_r of 170 kDa, whereas the predicted M_r is 134 kDa. Figure 3.3 shows two representative blots for Egfr at two

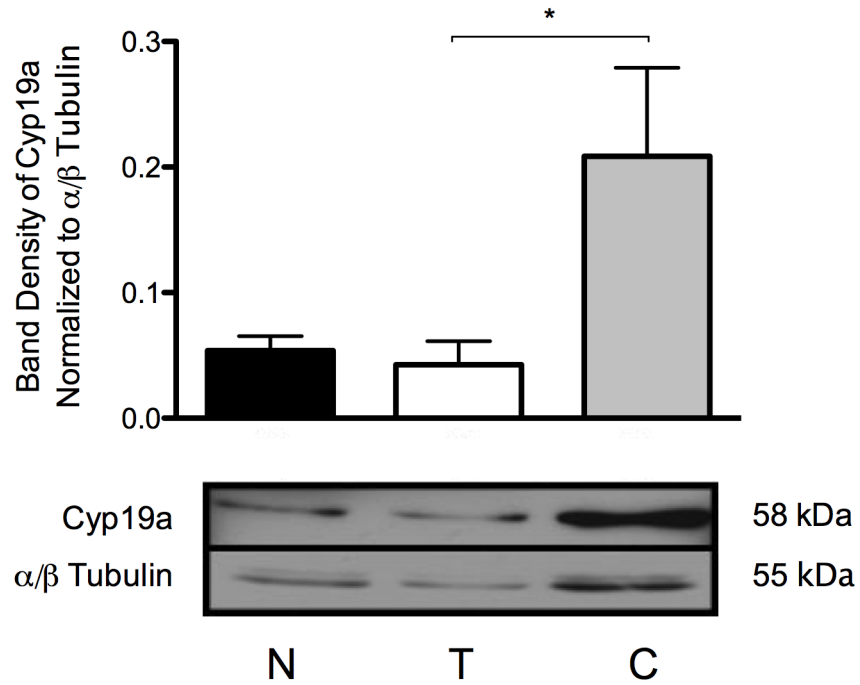


Figure 3.1 Quantitative representation and immunoblot analysis of Cyp19a
 Quantitative representation and immunoblot of Cyp19a expression in normal ovaries (N), JGCTs (T) and COV434 cell lysates (C) normalized to α/β Tubulin. [* represents statistical significance ($p \leq 0.05$)]. A quantity of 20 μ g of protein was loaded in each lane. n = 6 individual samples.

different exposure times, with the loading control β -actin used to normalize the relative expression for each individual sample. Egfr was significantly overexpressed in mouse GCTs, with a mean 10-fold increase when compared with the normal, whole ovary ($p = <0.0001$) and COV434 sample lysates ($p = 0.0007$). No difference was observed between normal, whole ovaries and the COV434 cell line. With equivalent protein loading, increased exposure time was required for Egfr band detection in the normal ovary and COV434 lysates and no significant difference was observed (Figure 3.4).

Esr2

Esr2 expression was examined in normal whole ovaries, mouse GCT specimens and COV434 cell lysates by immunoblotting, using a polyclonal antibody with cross-species reactivity. Figure 3.5 shows a representative blot of Esr2 with the loading control α/β Tubulin used to normalize the relative expression for each individual sample. Esr2 exhibited a M_r of 56 kDa, as per the expected molecular weight for Esr2. The quantitative densitometric analysis showed a 2-fold reduction in the expression of Esr2 expression between normal, whole ovary and GCT lysates ($p = <0.0001$), with a further 2-fold reduction between GCTs and COV434 lysates ($p = <0.0001$). A significant decrease was also observed between normal, whole ovary and COV434 lysates ($p = <0.0001$; $n = 6$).

Foxl2

The presence of Foxl2 expression in normal whole ovaries, mouse GCT specimens and COV434 cell lysates was evaluated by immunoblotting using a polyclonal antibody suitable for cross-species detection. Immunoblot using the Foxl2 primary antibody

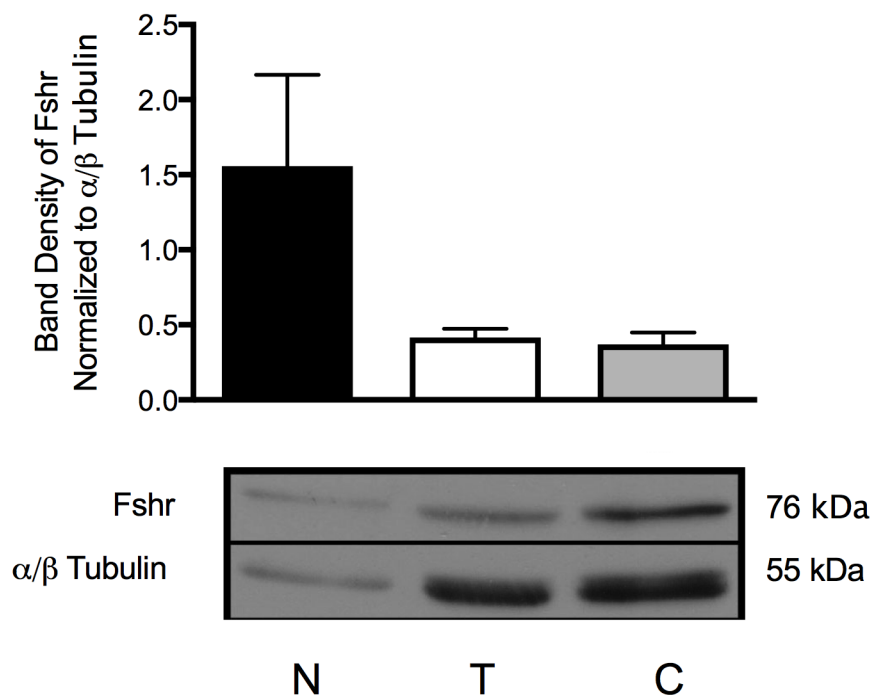


Figure 3.2 Quantitative representation and immunoblot analysis of Fshr

Quantitative representation and immunoblot of Fshr expression in normal ovaries (N), JGCTs (T) and COV434 cell lysates (C) normalized to α/β Tubulin. A quantity of 30 μ g of protein was loaded in each lane. n=5 individual samples.

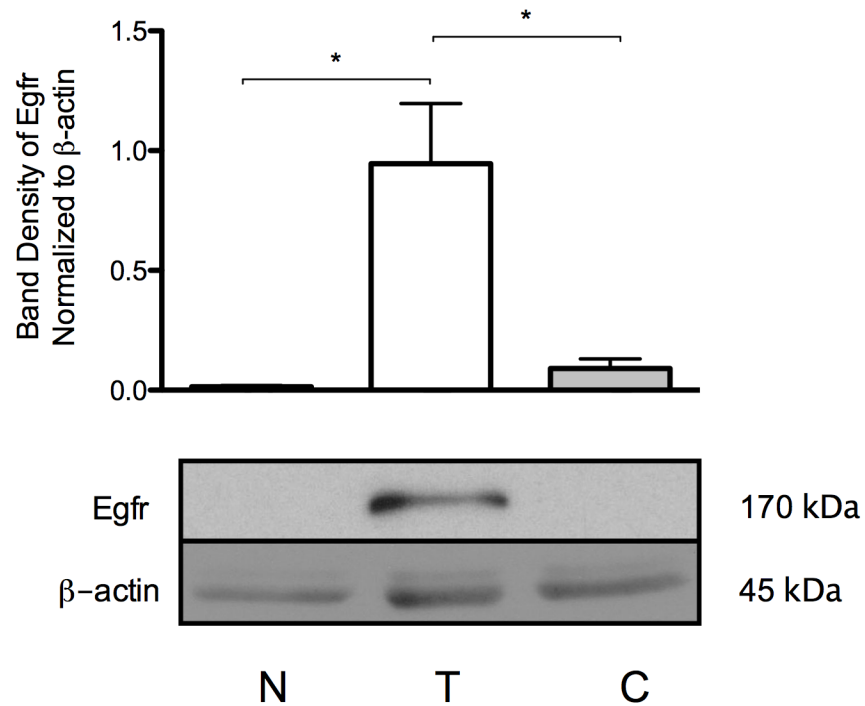


Figure 3.3 Quantitative representation and immunoblot analysis of Egfr

Quantitative representation and immunoblot of Egfr expression in normal ovaries (N), JGCTs (T) and COV434 cell lysates (C) normalized to β -actin. [* represents statistical significance ($p \leq 0.05$)]. A quantity of 30 μ g of protein was loaded in each lane. n=6 individual samples.

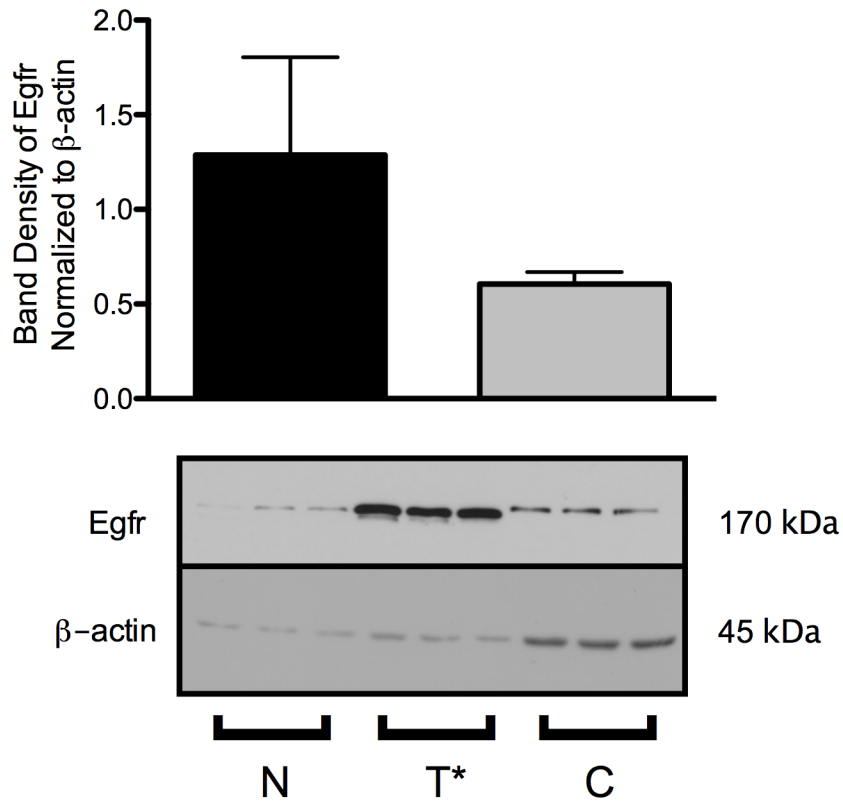


Figure 3.4 Quantitative representation and immunoblot analysis of Egfr

Quantitative representation and immunoblot of Egfr expression in normal ovaries (N), and COV434 cell lysates (C) with increased exposure time normalized to β -actin. JGCT (T) samples were not analyzed due to overexposure. A quantity of 30 μ g of protein was loaded in each lane. n=3 individual samples.

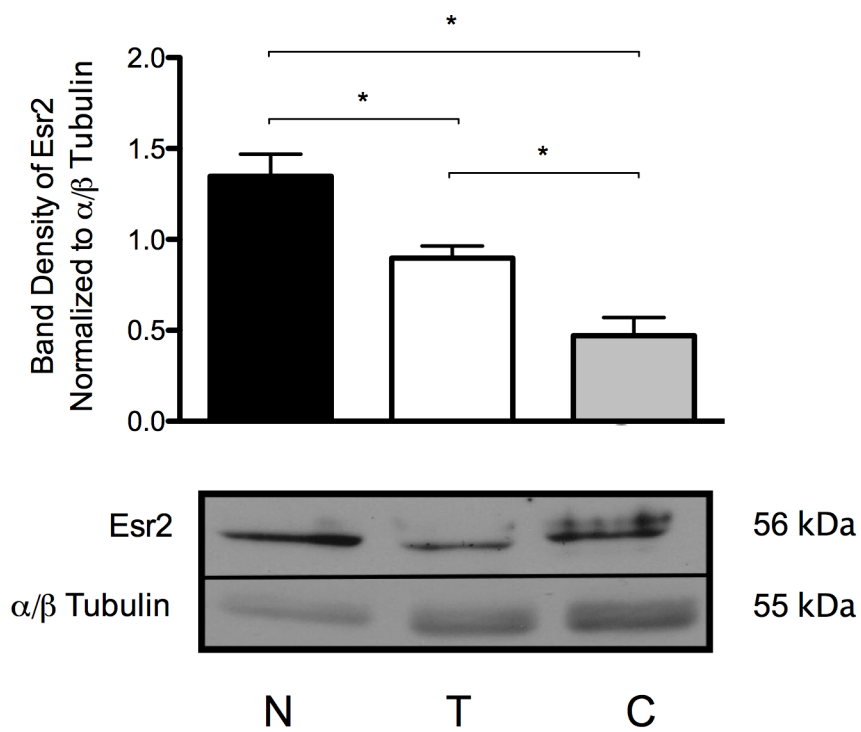


Figure 3.5 Quantitative representation and immunoblot analysis of Esr2

Quantitative representation and immunoblot of Esr2 expression in normal ovaries (N), JGCTs (T) and COV434 cell lysates (C) normalized to α/β Tubulin. [* represents statistical significance ($p \leq 0.05$)]. A quantity of 30 μ g of protein was loaded in each lane. n=6 individual samples.

exhibited a M_r of 38 kDa as per the expected molecular weight for Foxl2. Figure 3.6 shows a representative blot of Foxl2 with the loading control α/β Tubulin used to normalize the relative expression for each individual sample. Quantitative densitometric analysis showed no significant difference in the expression of Foxl2 was found between the three experimental groups (n = 5).

Sox9

Sox9 expression was examined in normal whole ovaries, mouse GCT specimens and COV434 cell lysates by immunoblotting, using a polyclonal antibody with cross-species reactivity (H90, Santa Cruz Inc., Santa Cruz CA). Immunoblotting revealed a band at a M_r of 65 kDa, whereas the predicted molecular weight for Sox9 is 56 kDa; however the same molecular weight band was detected in a positive tissue control lysate prepared from male mouse prostate gland suggesting a slight variation in size. Figure 3.7A shows the representative blot of Sox9 with the loading control α/β Tubulin used to normalize the relative expression for each individual sample. Quantitative densitometric analysis of the mean band density indicated that Sox9 was expressed approximately 10-fold higher in the GCT samples when compared with the normal, whole ovaries ($p = 0.0113$; $n = 6$) and approximately 20-fold higher relative to the COV434 cell lysates ($p < 0.0001$; $n = 6$). Unlike all the other proteins examined so far that have a predicted expression profile for female ovarian tissues, Sox9 is an important regulator of male gonad development and the high expression observed in mouse GCTs was unexpected. Therefore, this finding was investigated further with another monoclonal antibody for Sox9 (D8G8H, Cell

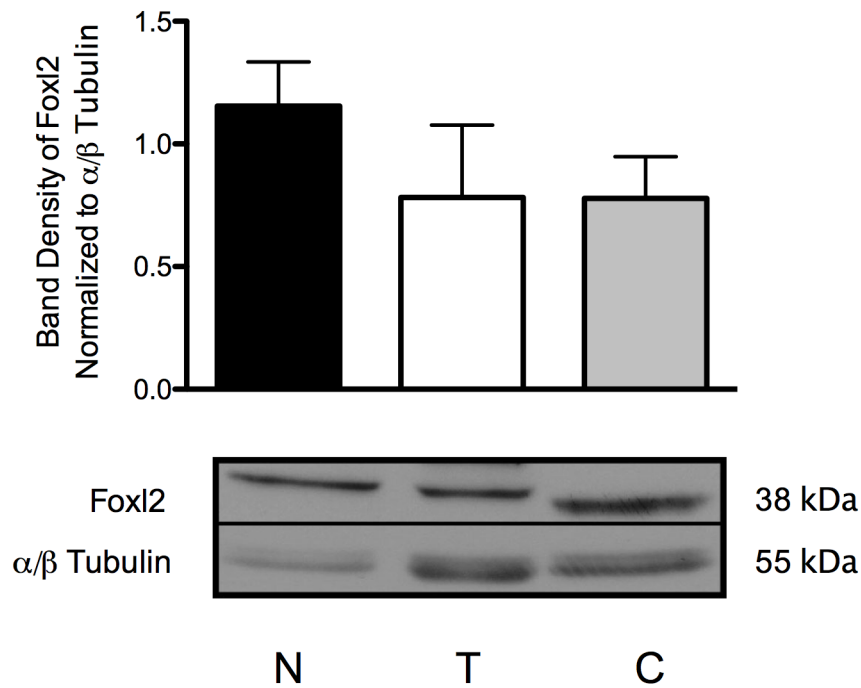


Figure 3.6 Quantitative representation and immunoblot analysis of Foxl2

Quantitative representation and immunoblot of Foxl2 expression in normal ovaries (N), JGCTs (T) and COV434 cell lysates (C) normalized to α/β Tubulin. A quantity of 30 μ g of protein was loaded in each lane. n=5 individual samples.

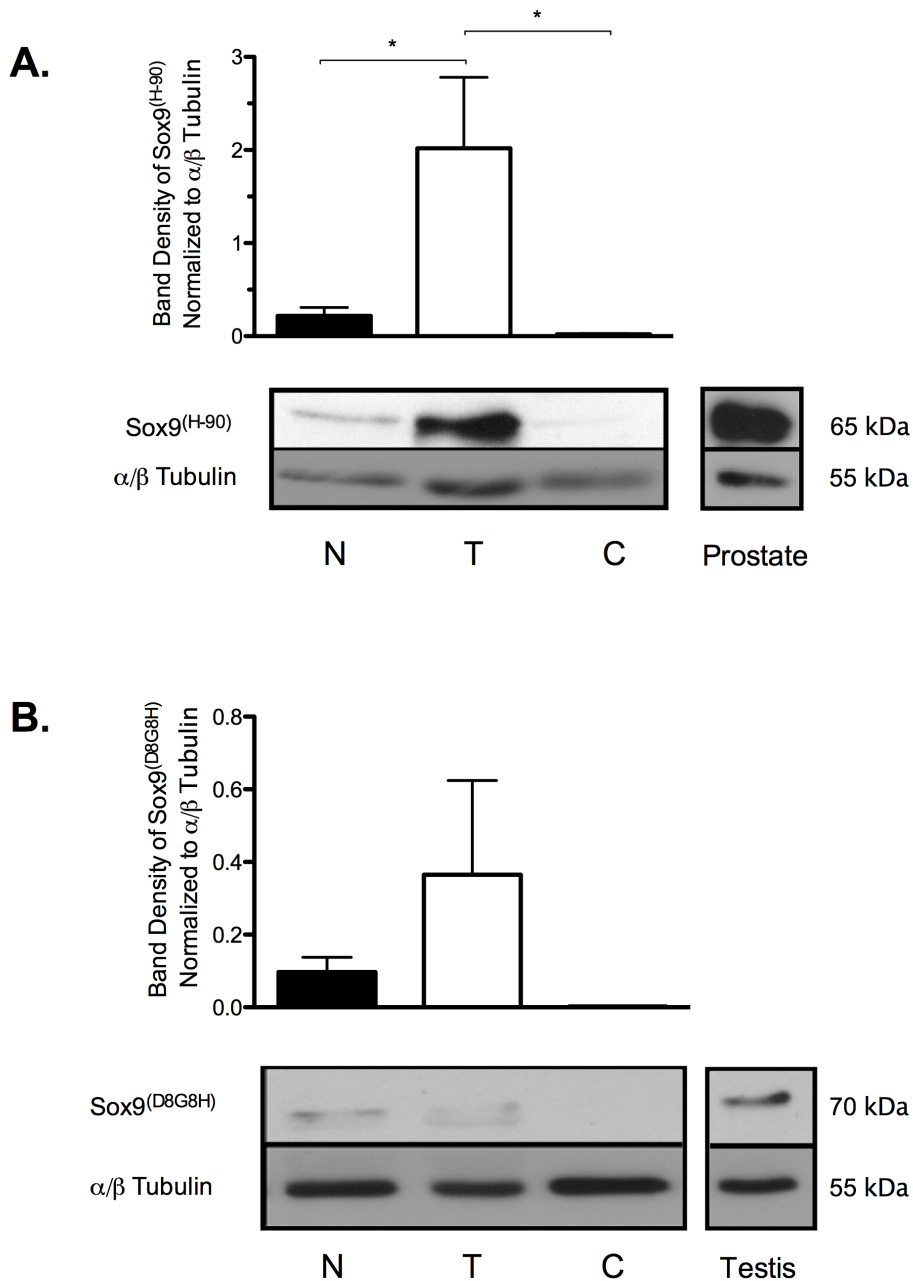


Figure 3.7 Quantitative representation and immunoblot analysis of Sox9

Quantitative representation and immunoblot of Sox9 expression in normal ovaries (N), JGCTs (T) and COV434 cell lysates (C) normalized to α/β Tubulin (A & B), mouse prostate (A) and testis (B) for a relative comparison of intensity of expression. A polyclonal Ab (H90; A) and monoclonal Ab (D8G8H; B) confirmed expression. [* represents statistical significance ($p \leq 0.05$)]. A quantity of 30 μg of protein was loaded in each lane. n=6 individual samples (A), n=4 individual samples (B).

Signaling Technology, Danvers MA) useful for immunoblotting and IHC between mouse and human tissues.

Figure 3.7B shows the representative immunoblot for Sox9 expression in matched normal ovary and GCT lysates to those examined in Figure 3.7A, but using the monoclonal Sox9 antibody (n = 4). For these immunoblots, fresh lysates were prepared for the COV434 cell line (n = 4) and male mouse testis was used to prepare a positive tissue control for Sox9 expression for both immunoblotting and IHC. No significant difference was observed between the three groups however, this could be due to the small sample size and there is a trend for consistent expression in Figure 3.7A and 3.7B. In Figure 3.7B, the intensity of the GCT expression is less than in Figure 3.7A and Sox9 expression is present in the normal ovaries. Sox9 was not detected in the COV434 cell line using either the polyclonal or the monoclonal antibody.

3.2 Immunohistochemical Analysis

In Figure 3.8, the presence of Sox9 expression in normal whole ovaries (A) and testis control tissue (B) was evaluated by IHC. Figure 3.8A shows the normal whole ovaries with H and E staining at 5X magnification, the IgG antibody control stained tissue (inset), and the Sox9 stained tissue at 10X magnification and 20X magnification. Figure 3.8B shows the testis control tissue with H and E staining at 5X magnification, the IgG antibody control stained tissue (inset), and the Sox9 stained tissue at 10X magnification and 20X magnification. In the testis, a specific Sox9 staining is evident in the Sertoli cells, as expected. In the normal ovary sections, stromal cells, possibly thecal cells, of uncertain identity surrounding growing follicles show positive Sox9 staining, although GC cells in all follicle stages were negative for Sox9 expression.

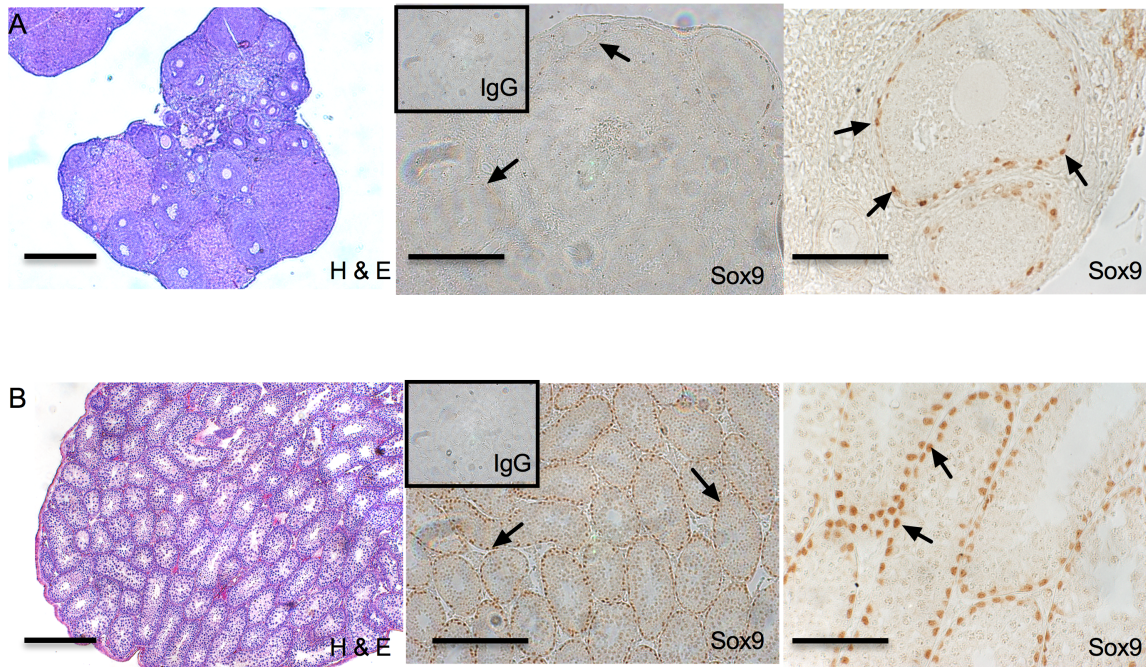


Figure 3.8 IHC of normal gonad condition

IHC analysis of normal whole ovaries (A) and normal testis tissue (B) from mice. H&E staining is at a magnification of 5X (Scale bar = 100 μm). The inset shows IgG control staining at 10X magnification. Sox9 staining is shown at magnifications of 10X (Scale bar = 50 μm) and 20X (Scale bar = 20 μm), respectively. Arrows shows areas positive for Sox9 staining.

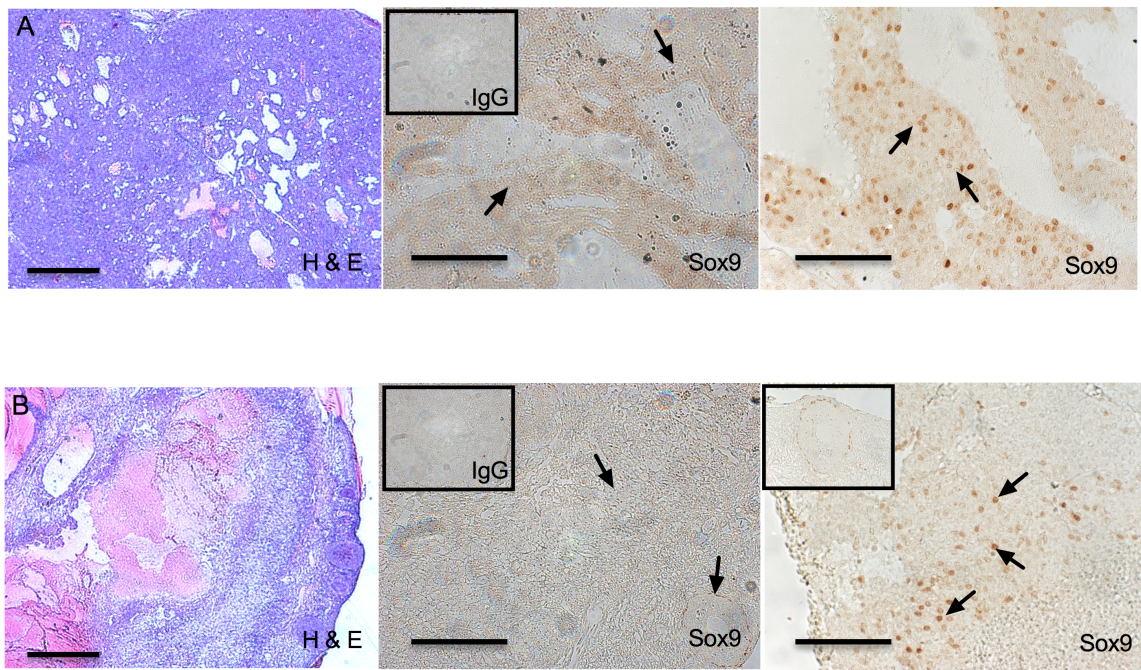


Figure 3.9 IHC of JGCTs from SWR background mice

IHC analysis of two unique JGCTs (A & B) from SWR background mice. H&E staining is at a magnification of 5X (Scale bar = 100 μm). The inset shows IgG control staining at 10X magnification. Sox9 staining is shown at magnifications of 10X (Scale bar = 50 μm) and 20X (Scale bar = 20 μm), respectively. In B, for Sox9 staining at 20X, the inset shows an intact follicle in the GCT showing the same staining pattern as in Figure 3.8A. Arrows shows areas positive for Sox9 staining.

Figure 3.9 shows two unique GCT specimens with H and E staining at 5X magnification, the IgG antibody control stained tissue (inset), and the Sox9 stained tissue at 10X magnification and 20X magnification. Clusters of Sox9 positive cells are present in proliferative (non-necrotic) regions of both GCTs, although expression is not consistent throughout the tumour mass. The contribution of Sox9 expressing cells in the normal ovaries and the GCTs support the detection of a band following immunoblotting of the ovary and GCT tissue lysates.

4.0 Discussion

Overview

GCTs can be classified as either adult or juvenile subtypes based on the age of onset and histology, affecting girls and women at both ends of the female reproductive spectrum. Although the adult subtype has been classified in humans by a consistent somatic mutation in the *FOXL2* gene, as of yet, no altered gene or protein has been identified as a consistent molecular feature for the JGCT type (Shah *et al.* 2009). The COV434 cell line established from a human GCT retains features of normal GC but does not possess the AGCT-associated mutation in *FOXL2*, rendering it as a frequently used model for JGCT (Zhang *et al.*, 2000). Early-onset GCTs appear in females of the SWR inbred strain driven by heritable susceptibility loci on Chr 4 and Chr X, as a model of JGCT development that is independent of *Foxl2* genetic variation on mouse Chr 9 (Smith *et al.*, unpublished). To compare these two JGCT model systems, I examined the expression of six essential proteins related to normal mammalian gonadal development and reproductive function: *Cyp19a*, *Egfr*, *Esr2*, *Foxl2*, *Fshr* and *Sox9*. Each protein examined was assessed by immunoblotting in individual mouse GC tumours compared to normal whole ovaries from female mice of the same young age and strain background, as well as lysates derived from the COV434 human cell line. Although GCs represent a major contributing cell type to the young ovary and the mouse GCTs, the sampling of whole mouse ovaries and GCTs to create mixed protein lysates is one limitation of this study due to the heterogeneity of cell types present. To address this limitation for *Sox9* specifically, IHC was performed for *Sox9* expression in the normal mouse ovary and unique mouse GCTs, to identify the *Sox9* expressing cells. Overall, the objective of this thesis was to determine how similar the protein profile is the normal mouse ovaries,

mouse GC tumours and the COV434 line to provide leads for proteins and genes that may be commonly expressed, as foundation for further translation of candidate proteins or gene expression as the mapped SWR *Gct* susceptibility loci are investigated in the human COV434 cell line for gene-coding or regulatory variants that trigger early onset tumourigenesis.

4.1 SWR mouse strain GC tumours and the normal ovarian condition

Spontaneous GCTs are rare in the human condition, with JGCTs even more rare than AGCTs, making the determination of their unique etiology challenging (Young *et al.*, 1984). If the SWR mouse model for spontaneous, early-onset GC tumours is a translational model for the human JGCT condition, there is a developmental window, a genetic susceptibility and an endocrine trigger that must all come together for GC tumours to initiate (Beamer *et al.*, 1985, Tennent *et al.*, 1990). The initiation of GC tumours during the brief developmental window in SWR female mice between the ages of 3 to 4 wks suggests an early alteration present from birth, with strong influence of heritable genetic factors influence the mouse model (Tennent *et al.*, 1990). The normal ovary provides a baseline to compare the protein profile to individual GC tumours, being collected from genetically identical and age-matched mice; this is a more representative overview of the acquired GCT changes. In addition, by sampling the GCTs at the earliest possible time point when they are macroscopically visible (approximately 6 wks of age), the number of acquired mutations represented in the proteome is predicted to be low, indicating that any changes would have likely occurred at the time of tumour initiation. By looking at the expression of proteins essential for normal reproductive development

and function, insight into probable initiators in the early stages of the reproductive systems development can be gained.

Each protein of interest has an established knowledge base in the current literature; however, little is known about their status in the rare JGCT condition. To establish a profile of confirmed GCTs from SWR mice, we compared them to the normal whole ovaries of unaffected female littermates. Proteins involved in the normal physiological processes of the ovary, such as Cyp19a, Fshr and Egfr provided a starting point of investigation.

In age matched GCTs, Cyp19a (aromatase) and Fshr remained unchanged from their normal ovary controls, with a wide variation in the normal ovaries for Fshr, which could be to expression differences between individual mice due to their normal estrus cycles. This result was anticipated, since Cyp19a is upregulated by Fsh activation through the Fshr on the GC population and by regulation of Cyp19a by the transcription factor Foxl2 (Fleming *et al.* 2010). More support for sufficient Cyp19a expression in GCTs is the observation by Beamer *et al.* (1985) that the mice who develop the tumours are highly estrogenized, supported by the observation of thickened uteri, enlarged vaginal opening and a solid, large cervix. This indicates that Cyp19a is at a level that allows for continued E₂ production.

Another physiologically relevant protein of the ovary is Egfr, which was investigated by immunoblotting and compared between age-matched ovaries and individually collected, spontaneous GCTs. Egfr is expressed in normal mouse ovaries where it plays a role in the FSH pathway to stimulate folliculogenesis, leading to follicle recruitment (Hunzicker-Dunn & Maizels, 2006). A very significant up-regulation of Egfr

protein was measured in isolated protein lysates from early onset GCTs extracted from SWR-derived female congenic mice compared to normal ovary pairs from the littermate controls (Figure 3.3). Up-regulation of Egfr was consistent across individual mouse GCTs, to the point that equivalent protein loading led to signal saturation in the GCTs with minimal signal in the normal ovary at the equivalent exposure time (Figure 3.4). In the current study, blots are shown with minimal exposure for the intense JGCT bands and at a higher exposure for the normal ovaries and COV434 lysates (Figure 3.3 & Figure 3.4, respectively). For future work it would be beneficial to load a proportion of the JGCT lysates to be able to analyze all samples at the same exposure time. In a previous study done with SWR mice, Tennent *et al.* (1989) found increased Egfr in GCTs compared to normal ovaries by a qualitative assessment of antibody-mediated immunofluorescence, as well as measuring EGF ligand binding capacity and proliferative response of short-term cultured tumour cells to EGF. My findings agree with the report of Tennent *et al.*, regarding SWR-derived JGCTs observing a 10-fold increase in Egfr expression in JGCTs compared with normal ovary pairs. These results also agreed with general literature of Egfr, which indicates the overexpression, and upregulation of the protein in many types of cancers (Tennent *et al.* 1989, Andersson *et al.*, 2014, Higgins *et al.*, 2014). In this study, global Egfr expression was investigated; however, subtypes of Egfr have been indicated in other types of cancers, such as HER2 in breast cancer (Leibl *et al.* 2006). Using a global Egfr antibody only allowed for the investigation of all receptor subtypes (Her-1, Her-2, Her-3 and Her-4) but not the ligands of Egfr. By only investigating the global Egfr expression rather than the specific subtypes, I was unable to determine which subtypes specifically could be involved in the upregulation of Egfr in

JGCTs, limiting our specific knowledge of the tumours and possible treatment options. However, the dramatic upregulation in our tumour samples suggest an anti-EGFR therapy may be a viable option for JGCT.

Another group of proteins that were investigated included Foxl2, Esr2 and Sox9. Foxl2 and Sox9 are important for normal gonad specification in the female ovary and male testis, respectively, with expression patterns that are characteristically mutually exclusive, such that somatic cells of the developing gonads express only one or the other of these sex specification factors (Tanaka *et al.* 2014). Esr2 also plays an important role in ovarian specification and is the primary Er isoform expressed in ovarian GCs (Uhlenhaut *et al.*, 2009).

Based on prior knowledge of *FOXL2* somatic mutation status in human AGCTs and consideration of the variation in overall expression status of wildtype *FOXL2* in JGCTs, it was important to determine Foxl2 protein expression levels in the SWR derived tumours compared to the normal condition (Shah *et al.*, 2009; Jamieson *et al.*, 2010). In my investigation comparing protein lysates from normal ovary pairs to age-matched and genetic strain matched mouse GCTs, Foxl2 protein expression showed no significant difference between tumour samples and normal samples, demonstrating agreement between our mouse model and a proportion of JGCTs identified that retain a normal degree of nuclear Foxl2 expression as GCs of a normal ovary (Kalfa *et al.*, 2007). One limitation of my study was the absence of IHC in mouse GCTs to confirm nuclear localization of the Foxl2 transcription factor. Matched samples of GCTs isolated for protein lysates were retained for IHC purposes, but the chosen method of fixation in paraformaldehyde (4 %) led to non-specific staining with IgG control antibody in two

different IHC protocols, with or without antigen retrieval (data not shown). Follow up experiments using optimized IHC fixation is required to confirm nuclear Foxl2 localization in the mouse GCTs.

Kalfa *et al.* (2007) made the suggestion that retention of nuclear FOXL2 protein is associated with a less aggressive tumour presentation, although additional cohorts and clinical follow up would help support this conclusion. At the early sampling stage of mice aged 6 wks, only 2 -3 wks following GCT initiation at puberty, the mouse tumours sampled for protein lysates in this study are proliferative masses of GC tumour cells that have not yet acquired malignant properties. In the SWR mouse model, approximately half of the GCTs progress to hormone-independent growth and metastatic potential when the hosts are much older (> 6 months; Tennent *et al.*, 1990). It is a future direction for this study to compare the protein expression profiles of the early GCTs identified here with late primary tumours or metastatic GCT foci sampled from older female mice, to address the translational hypothesis that Foxl2 protein expression would be diminished or lost with advanced malignancy.

Esr2, historically known as Estrogen receptor β , is necessary for the normal reproductive functioning of the ovary and is highly expressed in the GCs (Nalvarte *et al.* 2016). Esr2 protein is an important developmental and physiological ovarian factor that showed a significant decrease in GCTs relative to lysates prepared from the normal mouse ovary. One of Esr2's important functions is to support female gonad specification by contributing to Sox9 transcriptional suppression during ovarian development (Uhlenhaut *et al.*, 2009). In terms of overall fertility phenotypes, Esr2 knockout mice are viable and the ovaries develop, but the females are subfertile compared to wildtype

controls due to a decrease in follicle maturation and ovulation (Couse *et al.*, 2006; Jayes *et al.* 2014). The majority of SWR female mice without pubertal onset GCTs have normal fertility and reproductive history, suggesting *Esr2* expression is sufficient in the unaffected ovaries (Dorward, unpublished). When both Estrogen receptor α (*Esr1*) and *Esr2* are deleted in engineered mouse strains, testis-like structures and Sertoli-like cells appear in the mouse ovary, suggesting a cooperative role of the Er signaling network to maintain GC identity; however, GC tumour susceptibility is not observed (Couse *et al.*, 1999). Reduced expression of *Esr2* in the SWR strain GCT samples suggests a tumour suppressor contribution of *Esr2*, with a potential influence on the androgen-sensitivity of the tumorigenic program (Beamer *et al.*, 1988; Tennent *et al.*, 1993; Dorward *et al.* 2007). IHC follow up of GCT tissues would also determine if remaining *Esr2* protein is mislocalized to the cytoplasm, contributing to imbalanced Er signaling.

During gonad specification, the *Foxl2* and *Sox9* transcription factors have prominent roles to support ovarian or testis development, respectively. Somatic cell expression of *Foxl2* and *Sox9* in the gonad is exclusive in this context, although some conditions can lead to a sex-specific switch of the gene expression profiles, where male-to-female or female-to-male changes are observed, such as the female-to-male cellular transdifferentiation observed in the *Esr1/Esr2* double knockout ovaries (Couse *et al.*, 1999). In the case of gonadal tumorigenesis, a population of *Foxl2*-expressing granulosa-like tumour cells may appear in the male testis that no longer express *Sox9*, as has been observed in several cases of Juvenile-type GCTs of the Testis (JGCTT; Kalfa *et al.*, 2008). Of note, male mice of the SWR strain do not exhibit gonadal stromal tumours

in general, or JGCTs specifically, indicating the *Get* loci have sex-specific influence to trigger early onset GCTs only in the female ovary.

The ovarian GCTs of SWR female mice had never been examined for Sox9 expression so I approached this initially using an immunoblotting strategy. The protein expression profile of GCTs showed a significant overexpression of Sox9 using a polyclonal antibody for Sox9, similar positive control tissue lysates prepared from the prostate gland of the mature male mouse reproductive tract with high Sox9 expression (Ma, F *et al.* 2016; Figure 3.7A). The intensity of Sox9 expression in GCT lysates was an interesting and novel finding that was further investigated with a monoclonal antibody to the Sox9 protein useful for both immunoblotting and IHC. A increase in Sox9 expression was observed in mouse GCTs relative to normal ovary protein lysates using the monoclonal antibody however it was not significant and testis as a control tissue to ensure the accuracy and confirm the initial result from the polyclonal antibody (Figure 3.7B).

To address the limitation of looking at expression levels in the heterogeneous whole, ovary and comparing it to the GCT protein lysates that also have some protein contributions from other cell populations (blood, immune cells, vascular endothelial cells, etc.). I investigated the localization of the Sox9 expression in normal ovaries and JGCTs from female SWR-background mice and testis control tissue from male mice by IHC using the monoclonal antibody. Figure 3.8A and Figure 3.8B show H&E staining of normal ovary and testis, as well as Sox9 staining of these tissues with IgG as a control. A normal staining pattern is visible in the Sertoli and Leydig cells of the testis as expected (Daigle *et al.* 2015). In the normal ovary, Sox9 staining was observed in some stromal

cells located in the outside perimeter of maturing follicles; however, the GCs in follicles of all stages were negative for Sox9 staining (Figure 3.7A). This small contribution of Sox9 positive cells in the ovary likely contributes to the minor representation of Sox9 detection in the normal ovary lysates with the immunoblotting technique (Figure 3.7B).

In addition to visualizing Sox9 expression in normal gonads, it was also explored in two additional JGCTs extracted from SWR-background female mice whose tissues were fixed in Bouin's solution, permitting specific Sox9 detection. Figure 3.9A and Figure 3.9B represent two independent JGCTs collected from female mice at 8 wks of age. H&E staining shows the highly cellular nature of the tumours as opposed to the well organized follicle population of the ovary, with the majority of the ovarian mass taken up by the GC cells. Although these specimens were collected at "early" time points post-initiation at 3-4 wks of age, some areas of necrosis are evident, where the GC proliferations presumably outpace vasculature development with restrictions to nutrient and oxygen supply. Sox9 expression was not consistent across the GCT, but was observed in a selection of cells throughout the two GCTs examined (Figure 3.9A & Figure 3.9B). There are several possibilities as to what these Sox9-positive tumour cells are and where they originated: 1) they may be the same Sox9-positive cells that were observed in the normal ovary but are now distributed throughout the GCT since the follicular structures are abolished; 2) due to leaky vasculature, the Sox9-positive cells may have migrated from other areas into the tumour environment, or 3) it is quite possible that these cells are indeed a subset of GC tumour cells that are now expressing Sox9. Further exploration of this change in the expression of gonad specification factors of the mice is necessary to aid in the determination of GCT initiating factors such as

Gct1, the most influential tumour susceptibility locus identified in the SWR strain (Beamer *et al.*, 1998; Dorward *et al.*, 2005; Smith *et al.*, 2013). Based on the expression for somatic cells of the gonad to express either Sox9 or Foxl2 and not both, a follow up of Foxl2 staining by IHC analysis in these GCT specimens is warranted, in addition to the markers already examined such as Egfr, Fshr and Esr2 to identify the Sox9 expressing cells as potential GCT cells (Figure 1.2).

4.2 The normal ovary and a model human JGCT cell line, COV434

COV434 cells were obtained directly from a public repository and maintained at low passage number to generate lysates for my protein-profiling investigation. A comparison of the COV434 cell line to the normal ovary in mice provides information on the status of the cell line as representative of GC tumour origin, akin to published findings by other research groups. The expression of the proteins of interest between the two conditions displayed a similar protein profile in both groups. Cyp19a, Fshr, Egfr, Foxl2 and Sox9 in normal, whole ovaries all showed equivalent expression levels with the JGCT cell line (Figure 3.1-3.4, Figure 3.6); however, in contrast with other groups, a distinct band indicating FOXL2 expression was present in the COV434 cell line which will be further discussed in section 4.3. The only protein that had a significantly decreased expression in the COV434 cell line was Esr2 having a 4-fold decrease from the normal ovary (Figure 3.5); it was interesting that this pattern was similar to the mouse-derived GCTs, suggesting reduced Esr2 expression is important for JGCT tumorigenesis. The similarities in the expression levels of proteins important in GCs between normal, whole ovaries and the homogenous COV434 JGCT cell line helps to address the limitation of using the heterogeneous whole ovary, indicating that although

many cell types were present in the immunoblotting analysis, the comparable levels of the proteins with a GC specific cell line aids in the confirmation of GC specific expression in the whole ovary lysates.

4.3 The Mouse GC tumour and a model human GCT cell line, COV434

COV434 is an accepted JGCT cell line was used as a comparison to GCTs from the SWR mouse model to determine similarities and differences between the proteins of interest. The three physiological proteins investigated, CYP19A, FSHR and EGFR, varied in their comparison to the primary mouse GCTs. It is important to recognize that in both the mouse JGCTs and the COV434 cell line, some level of expression of the GC proteins of interest are present, but the expression levels may vary between the two models. An example of this is the expression of CYP19A; both primary GCT lysates and the COV434 cells have detectable CYP19A expression, which showed a significant upregulation in COV434 lysates when compared to the GCTs. It is unclear if this is a species-specific difference and our hypothesis that both models of JGCT would have a similar protein expression profile is not completely in disagreement with the observed results as there are many reasons for some of the quantitative differences. This result however is somewhat expected as it has previously been found that the human JGCT condition is characterized by increased E₂ production by the tumour, which is also noted in SWR female mice that have hormonally active GCTs, leading to premature menstruation indicating that the increase in CYP19A expression in the COV434 cell line leads to increased E₂ production in the human condition (Beamer *et al.*, 1988; Karalök *et al.* 2015). This increase in CYP19A expression supports my hypothesis that COV434 cells and JGCTs from SWR mice would have a similar expression profile. The only

protein from this group which had equivalent expression between GCTs and the COV434 lysates was FSHR.

One exception was the observation for EGFR, which had such a significant up-regulation in mouse GCTs. In terms of EGFR protein, a significantly lower expression was observed in the cells compared to the GCT samples (Figure 3.3), which had high overexpression and it appears to be not present at all when immunoblots were adequately exposed. In agreement with our hypothesis, that protein expression between the GCTs and COV434 cell line would be similar, was the expression of Fshr. Since we would predict that there would be little or no difference between the mouse GCTs and the representative human JGCT cell line, the absence of any change in FSHR expression in COV434 cells supported this prediction.

Of the three-gonad specification proteins studied, one protein that has been previously investigated in COV434 cells is FOXL2 due to the important role it plays in the development of the adult form of GC tumours. In previous studies, FOXL2 protein status was investigated and no expression was detected by IHC in the COV434 cell line (Jamieson *et al.*, 2010; Rosario *et al.* 2013). This did not agree with what I observed, which was FOXL2 expression in the cell line as well as in GCTs, with no significant difference between the two groups. The other two proteins, ESR2 and SOX9, both had a significant downregulation in the homogenous COV434 cell lysates relative to the primary mouse GCTs that are more heterogeneous in nature.

COV434 lysates were negative for SOX9 expression, with a significant band observed in the mouse GCT lysates. There was an intense expression observed at a higher M_r than what was expected from the polyclonal antibody product sheet (Santa Cruz, H90)

and was also higher than the expected M_r of Sox9. A faint band was also observed at the correct M_r compared to the stained protein ladder. To be convinced that this was just non-specific binding of the antibody and not Sox9 migrating at a higher M_r in human samples, a monoclonal Sox9 antibody (Cell Signaling Technology, D8G8H) was tested by immunoblotting as well as by IHC, confirming the specificity of the antibody and that the appropriate band was analyzed. The monoclonal Sox9 antibody was confirmed as highly specific by the staining pattern of the Sertoli cells of the testis after IHC. In addition to this experimental result, a literature search was performed and no reports of species-specific size differences were found.

ESR2 expression was significantly down-regulated in the COV434 lysates compared to the mouse GCT lysates whereas in normal ovaries, ESR2 was significantly higher. This down-regulation of ESR2 in the two GCT representative lysates may indicate a reduced expression of the tumour suppressor. To confirm the nuclear localization and functionality of the ESR2 protein, IHC or cell staining is needed in the future.

We would expect that the protein expression profile of the COV434 cell lysates and the JGCT samples to be similar as the cell line is representative of JGCTs, although species differences could have attributed to some of the quantitative differences in the mouse tumours and the human cell lysates. Although some expression differences in Cyp19a, Esr2, Egfr and Sox9 were observed in the COV434 cell lysates, the cell model is still considered in the literature and in this study to be representative of the human JGCT condition although perhaps not a perfect model of the disease. This characterization is supported by work done in IVF patients that provide evidence that the COV434 cell line

exhibit properties of GCs including the production of E₂ in response to FSH, as well as their ability to form connections with other cells around the oocyte (Zhang *et al.* 2000). With this evidence supporting the JGCT status of the cell line, it continues to be the best human model available. Unfortunately due to the rare nature of human JGCTs, accounting for only approximately 5 % of all GCTs, which are a rare subtype of ovarian cancer, a comparison of the COV434 cell line with primary human JGCTs has not been done to definitively determine its status. However, the expression status of several proteins of interest have been explored in human JGCTs. Over half of AGCTs and JGCTs surveyed were found to be positive for Egfr expression by IHC analysis (Leibl *et al.* 2006). Another protein that has been extensively studied in human JGCTs is FOXL2. One group who looked at human FOXL2 expression by IHC found expression to be normal in half of the cases they looked at while the other half, the more aggressive cases had absent or markedly reduced FOXL2 expression in human JGCTs (Kalfa *et al.* 2007). However, although some human samples were found to have normal FOXL2 expression, three other groups have also reported no or very low *FOXL2* gene expression in the COV434 cell line, in contrast to what I found by immunoblotting (Fleming *et al.*, 2010; Jamieson *et al.*, 2010; Rosario *et al.*, 2013). By comparing these two models, new insight into the actual source of the COV434 cell line could be identified and possibly investigated in the future. If COV434 is indeed a JGCT cell line, as reported, other factors can be contributing to the differences we have seen. Besides species variations, the cell line may have new adaptations to its artificial environment that tissue samples would not have acquired. To minimize these possible changes, the COV434 cell line was directly imported from the repository and expression levels were measured at a low

passage number to reduce the number of acquired changes. Another important distinction between the SWR JGCT samples and the COV434 cell line is the mouse tumours are identified as benign, non-metastatic lesions at the point of extraction; however, the COV434 cell line was developed from borderline malignant, metastatic lesion, which may have acquired a unique protein expression signature from the primary patient tumour at the time of its initial occurrence that contributed to its later malignant, metastatic nature (Van Den Berg-Bakker *et al.*, 1993, Zhang *et al.*, 2000). A better comparison may be to sample the mouse GCTs at a later time point, when they are malignant (Tennent *et al.*, 1990) and have potentially developed alterations similar to what is observed in the COV434 cell line. There is little currently known about the protein expression profile of COV434 cells compared to the established SWR mouse model, thus much of what was observed was novel information and valuable for further investigation of both mouse and human JGCTs.

5.0 Summary

The SWR mouse model of juvenile GC tumourigenesis provides a valuable resource to study not only the genetics of JGCTs but also their protein expression profiles. By investigating the various proteins involved in both ovarian physiology and gonad specification, we were able to gain new insights into the developmental processes when tumour initiation occurs, such as the possible alterations to the factors involved in the normal progression of the bipotential gonad formation to the ovaries indicated by the downregulation of *Esr2* and presence of *Sox9* positive cells that need to be investigated as bystander cells, or GC cells that have exchanged *Foxl2* expression for *Sox9* during the tumourigenic transition. In addition to new information, we were also able to confirm

what others have previously observed, for instance an increase of Egfr expression in GCTs. We were also able to confirm normal status of Cyp19a and Fshr between experimental groups. The comparison of GCTs to COV434 lysates provided new information about the status of Cyp19a, Egfr, Esr2 and Sox9, which we hypothesized to be similar but turned out to vary in their expression. Lastly, a comparison of the normal ovary of mice to the human COV434 cell line also showed many similarities that could be attributed to mutational status of the cell line or to species differences as with the GCT variability. This profile provides us with valuable insights into the status of JGCTs and is a good starting point to allow a basis for future investigations.

6.0 Future Directions

The next step in these investigations of JGCTs would be to continue building the protein expression profile of the tumour. Identification of other proteins of interest by looking at targets potentially altered upstream of Esr2 and Sox9 and then performing immunoblotting to determine protein expression levels and IHC of all proteins of interest to visualize the localization of each protein to their specific cell type would build on the knowledge we have gained here to investigate the potential effect on bipotential gonad development. Also, by performing IHC to confirm cell types that are Sox9-positive by looking at proteins specific to each cell type, for example Cyp19a in GCs and Cy17a1 in TCs. With the theory of two follicle waves, it is possible that follicles that develop GCTs come from the first wave of follicles, which have a limited contribution to reproductive fertility, and these follicles have lower Esr2 expression, whereas the second wave, which are the primary source of fertility, have normal Esr2 expression (Zheng *et al.*, 2014). Further exploration of these specific follicle populations by sampling GCTs at early and

late developmental timepoints and tracking cellular populations by IHC would provide valuable insights into the origin of JGCTs. Also, to further address the limitations of using whole ovaries, isolation of GCs and culture of those cells to look specifically at that cellular population would provide more specific details about their protein expression profile.

In addition to the protein profile, investigating any genetic alterations in the factors explored for protein expression could aid in the narrowing of candidates for *Gct1*. An interesting experiment to expand our knowledge of how the mouse JGCTs compare to the human condition would be to sample malignant tumours in the mice, by sampling a later time point and performing IHC to visualize the localized protein expression of specific tumour-initiating follicles, specifically looking at the three proteins that had extreme profiles; *Esr2*, *Egfr* and *Sox9*. A focused technique such as this would aid in the establishment of differences in tumour status that contribute to the differences we observed. *Egfr* can also be investigated further by doing more targeted expression analysis looking at subtypes including Her-1 and Her-2, especially those that are indicated in other cancers, leading to possible treatment options. Another interesting angle would be to look at the upstream enzyme of *Cyp19a*, 3β -HSD, to investigate its status that could lead to the buildup of androgens that lead to tumour development (JGCTs are androgen sensitive).

7.0 References

- Adashi, E. Y. (1994). Endocrinology of the ovary. *Human Reproduction*, 9(4), 815-827.
- Al-Agha, O. M., Huwait, H. F., Chow, C., Yang, W., Senz, J., Kalloger, S. E., Gilks, C. B. (2011). FOXL2 is a sensitive and specific marker for sex cord-stromal tumors of the ovary. *The American Journal of Surgical Pathology*, 35(4), 484-494.
- Andersson, N., Anttonen, M., Färkkilä, A., Pihlajoki, M., Bützow, R., Unkila-Kallio, L., & Heikinheimo, M. (2014). Sensitivity of human granulosa cell tumor cells to epidermal growth factor receptor inhibition. *Journal of Molecular Endocrinology*, 52(2), 223-234.
- Bast, R. C. Jr., Hennessy, B., & Mills, G. B. (2009). The biology of ovarian cancer: new opportunities for translation. *Nature Reviews. Cancer*, 9(6), 415-428.
- Beamer, W. G., Hoppe, P. C., & Whitten, W. K. (1985). Spontaneous malignant granulosa cell tumours in ovaries of young SWR mice. *Cancer Research*, 45, 5575-5581.
- Beamer, W. G. (1986). Gonadotropin, steroid, and thyroid hormone milieu of young SWR mice bearing spontaneous granulosa cell tumors. *Journal of the National Cancer Institute*, 77(5), 1117-1123.
- Beamer, W. G., Shultz, K. L., & Tennent, B. J. (1988a). Induction of ovarian granulosa cell tumors in SWXJ-9 mice with dehydroepiandrosterone. *Cancer Research*, 48(10), 2788-2792.
- Beamer, W. G., Tennent, B. J., Shultz, K. L., Nadeau, J. H., Shultz, L. D., & Skow, L. C. (1988b). Gene for ovarian granulosa cell tumor susceptibility, gct, in SWXJ recombinant inbred strains of mice revealed by dehydroepiandrosterone. *Cancer Research*, 48(18), 5092-5095.
- Beamer, W. G., Shultz, K. L., Tennent, B. J., & Shultz, L. D. (1993). Granulosa cell tumorigenesis in genetically hypogonadal-immunodeficient mice grafted with ovaries from tumor-susceptible donors. *Cancer Research*, 53(16), 3741-3746.
- Beamer, W. G., Shultz, K. L., Tennent, B. J., Azumi, N., & Sundberg, J. P. (1998a). Mouse model for malignant juvenile ovarian granulosa cell tumors. *Toxicologic Pathology*, 26(5), 704-710.
- Beamer, W. G., Shultz, K. L., Tennent, B. J., Nadeau, J. H., Churchill, G. A. & Eicher, E. M. (1998b). Multigenic and imprinting control of ovarian granulosa cell tumorigenesis in mice. *Cancer Research*, 58(16), 3694-3699.
- Benayoun, B. A., Caburet, S., Dipietromaria, A., Georges, A., D'Haene, B., Pandaranayaka, P. J. E., Veitia, R. A. (2010). Functional exploration of the adult

- ovarian granulosa cell tumor-associated somatic FOXL2 mutation p.Cys134Trp (c.402C>G). *PLoS ONE*, 5(1)
- Biggers, J. D., Finn, C. A., & McLaren, A. (1962). Long-term reproductive performance of female mice. I. effect of removing one ovary. *Journal of Reproduction and Fertility*, 3, 303-312.
- Bjorkholm, E., & Silfversward, C. (1981). Prognostic factors in granulosa-cell tumors. *Gynecologic Oncology*, 11(3), 261-274.
- Boyer, A., Goff, A. K., & Boerboom, D. (2010). WNT signaling in ovarian follicle biology and tumorigenesis. *Trends in Endocrinology Metabolism*, 21(1), 25-32.
- Canadian Cancer Society. (2015). Canadian Cancer Statistics. *Government of Canada*.
- Casagrande, J. T., Louie, E. W., Pike, M. C., Roy, S., Ross, R. K., & Henderson, B. E. (1979). "Incessant ovulation" and ovarian cancer. *Lancet*, 2(8135), 170-173.
- Chassot, A. A., Ranc, F., Gregoire, E. P., Roepers-Gajadien, H. L., Taketo, M. M., Camerino, G., . . . Chaboissier, M. C. (2008). Activation of beta-catenin signaling by Rspo1 controls differentiation of the mammalian ovary. *Human Molecular Genetics*, 17(9), 1264-1277.
- Chen, H., Palmer, J. S., Thiagarajan, R. D., Dinger, M. E., Lesieur, E., Chiu, H., Schulz, A., Spiller, C., Grimmond, S. M., Little, M. H., Koopman, P., & Wilhelm, D. (2012). Identification of novel markers of mouse fetal ovary development. *PLoS One*, 7(7): e41683.
- Colombo, N., Parma, G., Zanagnolo, V., & Insinga, A. (2007). Management of ovarian stromal cell tumors. *Journal of Clinical Oncology : Official Journal of the American Society of Clinical Oncology*, 25(20), 2944-2951.
- Couse, J.F., Hewitt, S.C., Bunch, D.O., Sar, M., Walker, V.R., Davis, B.J., and Korach, K.S. (1999). Postnatal sex reversal of the ovaries in mice lacking estrogen receptors alpha and beta. *Science* 286, 2328–2331.
- Couse, J. F., Yates, M. M., Rodriguez, K. F., Johnson, J. A., Poirier, D., & Korach, K. S. (2006). The intraovarian actions of estrogen receptor-alpha are necessary to repress the formation of morphological and functional Leydig-like cells in the femal gonad. *Endocrinology*, 147(8), 3666-3678.
- Crisponi, L., Deiana, M., Loi, A., Chiappe, F., Uda, M., Amati, P., . . . Pilia, G. (2001). The putative forkhead transcription factor FOXL2 is mutated in blepharophimosis/ptosis/epicanthus inversus syndrome. *Nature Genetics*, 27(2), 159-166.

- Daigle, M., Rournaud, P. & Martin, L. J. (2015). Expressions of Sox9, Sox5, and Sox13 transcription factors in mice testis during postnatal development. *Molecular and Cellular Biochemistry*, 407(1-2), 209-221.
- D'Angelo, E., Mozos, A., Nakayama, D., Espinosa, I., Catusus, L., Munoz, J., & Prat, J. (2011). Prognostic significance of FOXL2 mutation and mRNA expression in adult and juvenile granulosa cell tumors of the ovary. *Modern Pathology : An Official Journal of the United States and Canadian Academy of Pathology, Inc*, 24(10), 1360-1367.
- Dorward, A. M., Shultz, K. L., Ackert-Bicknell, C. L., Eicher, E. M., & Beamer, W. G. (2003). High-resolution genetic map of X-linked juvenile-type granulosa cell tumor susceptibility genes in mouse. *Cancer Research*, 63(23), 8197-8202.
- Dorward, A. M., Shultz, K. L., Horton, L. G., Li, R., Churchill, G. A., & Beamer, W. G. (2005). Distal Chr 4 harbors a genetic locus (Gct1) fundamental for spontaneous ovarian granulosa cell tumorigenesis in a mouse model. *Cancer Research*, 65(4), 1259-1264.
- Dorward, A. M., Shultz, K. L., & Beamer, W. G. (2007). LH analog and dietary isoflavones support ovarian granulosa cell tumor development in a spontaneous mouse model. *Endocrine-Related Cancer*, 14(2), 369-379.
- Dorward, A. M., Yaskowiak, E. S., Smith, K. N., Stanford, K. L., Shultz, K. L., & Beamer, W. G. (2013). Chromosome X loci and spontaneous granulosa cell tumor development in SWR mice: epigenetics and epistasis at work for an ovarian phenotype. *Epigenetics*, 8(2), 184-191.
- Edson, M. A., Nagaraja, A. K., & Matzuk, M. M. (2009). The mammalian ovary from genesis to revelation. *Endocrine Reviews*, 30(6), 624-712.
- Eggers, S., Ohnesorg, T., & Sinclair, A. (2014). Genetic regulation of mammalian gonad development. *Nature Reviews Endocrinology*, 10(11), 673-683.
- Fathalla, M. F. (1971). Incessant ovulation--a factor in ovarian neoplasia? *Lancet*, 2(7716), 163.
- Finn, C. A. (2001). Reproductive ageing and the menopause. *The International Journal of Developmental Biology*, 45(3), 613-617.
- Fleming, N. I., Knowler, K. C., Lazarus, K. A., Fuller, P. J., Simpson, E. R., & Clyne, C. D. (2010). Aromatase is a direct target of FOXL2: C134W in granulosa cell tumors via a single highly conserved binding site in the ovarian specific promoter. *PLoS One*, 5(12), e14389.

- Fuller, P. J., Verity, K., Shen, Y., Mamers, P., Jobling, T., & Burger, H. G. (1998). No evidence of a role for mutations or polymorphisms of the follicle-stimulating hormone receptor in ovarian granulosa cell tumors. *The Journal of Clinical Endocrinology and Metabolism*, 83(1), 274-279.
- Georges, A., Auguste, A., Bessière, L., Vanet, A., Todeschini, A.L., & Veitia, R.A. (2013). FOXL2: a central transcription factor of the ovary. *The Journal of Molecular Endocrinology*, 52(1), R17-33.
- Gougeon, A. (2004). Dynamics of human follicular growth: Morphologic, dynamic, and function aspects. In P. Leung, & E. Y. Adashi (Eds.), *The ovary*.
- Hanley, N. A., Hagan, D.M., Clement-Jones, M., Ball, S. G., Strachan, T., Salas-Cortés, L., McElreavey, K., Lindsay, S., Robson, S., Bullen, P., Ostrer, H., & Wilson, D. I. (2000). *SRY*, *SOX9* and *DAX1* expression patterns during human sex determination and gonadal development. *Mechanisms of Development*, 91(1-2), 403-407.
- Higgins, P.A., Brady, A., Dobbs, S. P., Salto-Tellez, M., Maxwell, P. & McCluggage, W. G. (2014). Epidermal growth factor receptor (EGFR), HER2 and insulin-like growth factor-1 receptor (IGF-1R) status in ovarian adult granulosa cell tumours. *Histopathology*, 64, 633-638.
- Hirshfield, A. N. (1992). Heterogeneity of cell populations that contribute to the formation of primordial follicles in rats. *Biology of Reproduction*, 47, 466-472.
- Hirshfield, A. N. & DeSanti, A. M. (1995). Patterns of ovarian cell proliferation in rats during the embryonic period and the first three weeks postpartum. *Biology of Reproduction*, 53, 1208-1221.
- Huang, B., Wang, S., Ning, Y., Lamb, A. N., & Bartley, J. (1999). Autosomal XX sex reversal caused duplication of *SOX9*. *American Journal of Medical Genetics*, 87, 349-353.
- Hunzicker-Dunn, M. & Maizels, E. T. (2006). FSH signaling pathways in immature granulosa cells that regulate target gene expression: Branching out from protein kinase A. *Cellular Signalling*, 18(9), 1351-1359.
- Jamieson, S., Butzow, R., Andersson, N., Alexiadis, M., Unkila-Kallio, L., Heikinheimo, M., . . . Anttonen, M. (2010). The FOXL2 C134W mutation is characteristic of adult granulosa cell tumors of the ovary. *Modern Pathology*, 23(11), 1477-1485.
- Jamieson, S. & Fuller, P.J. (2012). Molecular pathogenesis of granulosa cell tumors of the ovary. *Endocrine Reviews*, 33(1), 109-144.

- Jamieson, S. & Fuller, P.J. (2015). Tyrosine kinase inhibitors as potential therapeutic agents in the treatment of granulosa cell tumors of the ovary. *International Journal of Gynecological Cancer*, 25(7), 1224-1231.
- Jamnongjit, M., Gill, A., & Hammes, S. R. (2005). Epidermal growth factor receptor signaling is required for normal ovarian steroidogenesis and oocyte maturation. *Proceedings of the National Academy of Sciences of United States of America*, 102(45), 16257-16262.
- Jayes, F. L., Burns, K. A., Rodriguez, K. F., Kissling, G. E. & Korach, K. S. (2014). The naturally occurring luteinizing hormone surge is diminished in mice lacking estrogen receptor beta in the ovary. *Biology of Reproduction*, 90(2), 24.
- Kalfa, N., Philibert, P., Patte, C., Ecochard, A., Duvillard, P., Baldet, P., Jaubert, F., Fellous, M., & Sultan, C. (2007). Extinction of *FOXL2* expression in aggressive ovarian granulosa cell tumors in children. *Fertility and Sterility*, 87(4), 896-901.
- Kalfa, N., Fellous, M., Boizet-Bonhoure, B., Patte, C., Duvillard, P., Pienkowski, C., Jaubert, F., Ecochard, A., & Sultan, C. (2008). Aberrant expression of ovary determining gene *FOXL2* in the testis and juvenile granulosa cell tumor in children. *The Journal of Urology*, 180, 1810-1813.
- Karalök, A., Taşçi, T., Üreyen, I., Türkmen, O., Öçalan, R., Şahin, G., Turan, T. & Tulunay, G. (2015). Juvenile granulosa cell ovarian tumor: clinicopathological evaluation of ten patients. *Journal of the Turkish-German Gynecological Association*, 16, 32-34.
- Kim, M.S., Hur, S.Y., Yoo, N.J., & Lee, S.H. (2010). Mutational analysis of *FOXL2* codon 134 in granulosa cell tumour of ovary and other human cancers. *Journal of Pathology*, 221(2), 147-152.
- Kitamura, S., Abiko, K., Matsumura, N., Nakai, H., Akimoto, Y., Tanimoto, H., & Konishi, I. (2017). Adult granulosa cell tumors of the ovary: a retrospective study of 30 cases with respect to the expression of steroid synthesis enzymes. *Journal of Gynecologic Oncology*, 28 (4).
- Knight, P. G., Satchell, L., & Glister, C. (2012). Intra-ovarian roles of activins and inhibins. *Molecular and Cellular Endocrinology*, 359(1-2), 53-65.
- Kobayashi, A. & Behringer, R.R. (2003). Developmental genetics of the female reproductive tract in mammals. *Nature Reviews Genetics*, 4(12), 969-980.
- Koonings, P. P., Campbell, K., Mishell, D. R., Jr, & Grimes, D. A. (1989). Relative frequency of primary ovarian neoplasms: A 10-year review. *Obstetrics and Gynecology*, 74(6), 921-926.

- Koopman, P., Gubbay, J., Collignon, J., & Lovell-Badge, R. (1989). Zfy gene expression patterns are not compatible with a primary role in mouse sex determination. *Nature*, 342(6252), 940-942.
- Koopman, P., Bullejos, M., & Bowles, J. (2001). Regulation of male sexual development by *sry* and *Sox9*. *Journal of Experimental Zoology*, 290, 463-474.
- Kurman, R.J. and Shih, I-M. (2011). Molecular pathogenesis and extraovarian origin of epithelial ovarian cancer. Shifting the paradigm. *Human Pathology*, 42(7), 918-931.
- Leibl, S., Bodo, K., Gogg-Kammerer, M., Hrzenjak, A. Petru, E., Winter, R., Denk, H., & Moinfar, F. (2006). Ovarian granulosa cell tumors frequently express EGFR (Her-1), Her-3, and Her-4: An immunohistochemical study. *Gynecologic Oncology*, 101(1), 18-23.
- Li, R., Phillips, D. M., Moore, A., & Mather, J. P. (1997). Follicle-stimulating hormone induces terminal differentiation in a predifferentiated rat granulosa cell line (ROG). *Endocrinology*, 138(7), 2648-2657.
- Lloyd, R.V. 2010. Endocrine Pathology: Differential diagnosis and molecular advances, Second Edition. *Springer Science & Business Media*, 318.
- Lunger, F., Vehmas, A. P., Fürnrohr, B.G., Sopper, S., Wildt, L., & Seeber, B. (2016). Opiate receptor blockade on human granulosa cells inhibits VEGF release. *Reproductive Biomedicine Online*, 32(3), 316-322.
- Ma, F., Ye, H., He, H. H., Gerrin, S. J., Chen, S., Tanenbaum, B. A., Cai, C., Sowalsky, A. G., He, L., Wang, H. Balk, S. P. & Yuan, X. (2016). Sox9 drives WNT pathway activation in prostate cancer. *The Journal of Clinical Investigation*, 126(5), 1745-1758.
- McGee, E. A., & Hsueh, A. J. (2000). Initial and cyclic recruitment of ovarian follicles. *Endocrine Reviews*, 21(2), 200-214.
- McLaren, A. (1991). Development of the mammalian gonad: The fate of the supporting cell lineage. *BioEssays : News and Reviews in Molecular, Cellular and Developmental Biology*, 13(4), 151-156.
- Mittwoch, U. (1992). Sex determination and sex reversal: genotype, phenotype, dogma and semantics. *Human Genetics*, 89(5), 467-479.
- Mork, L., Maatouk, D. M., McMahon, J. A., Guo, J. J., Zhang, P., McMahon, A. P., & Capel, B. (2012). Temporal differences in granulosa cell specification in the ovary reflect distinct follicle fates in mice. *Biology of Reproduction*, 86(2), 37.

- Nalvarte, I., Töhönen, V., Lindeberg, M., Varshney, M., Gustafsson, J.-A. & Inzunza, J. (2016). Estrogen receptor β controls MMP-19 expression in mouse ovaries during ovulation. *Reproduction*, *151*, 253-259.
- Netter, F. H., & Cochard, L. R. (2002). In Icon Learning Systems, Teterboro, N.J. (Ed.), *Netter's atlas of human embryology*. (pp. 177)
- Nishi, Y., Yanase, T., Mu, Y., Oba, K., Ichino, I., Saito, M., . . . Nawata, H. (2001). Establishment and characterization of a steroidogenic human granulosa-like tumor cell line, KGN, that expresses functional follicle-stimulating hormone receptor. *Endocrinology*, *142*(1), 437-445.
- Online Mendelian Inheritance in Man, OMIM[®]. Johns Hopkins University, Baltimore, MD. MIM Number: {110100}: {2014.19.11}: World Wide Web URL: <http://omim.org/>
- Pastuschek, J., Poetzsch, J., Morales-Prieto, D.M., Schleubner, E., Markert, U. R., & Georgiev, G. (2015). Stimulation of the JAK/STAT pathway by LIF and OSM in the human granulosa cell line COV434. *Journal of Reproductive Immunology*, *108*, 48-55.
- Pectasides, D., Pectasides, E., & Psyrri, A. (2008). Granulosa cell tumor of the ovary. *Cancer Treatment Reviews*, *34*(1), 1-12.
- Peters, H. (1969). The development of the mouse ovary from birth to maturity. *Acta Endocrinologica*, *62*, 98-116.
- Ramalingam, P. (2016) Morphogenic, immunophenotypic, and molecular features of epithelial ovarian cancer. *Oncology*, *30*(2), 166-176.
- Reuter, A.L., Goji, K., Bingham, N.C., Matsuo, M., and Parker, K.L. (2007). A novel mutation in the accessory DNA-binding domain of human steroidogenic factor 1 cause XY gonadal dysgenesis without adrenal insufficiency. *European Journal of Endocrinology*, *157*, 233-238.
- Riggins, G. J., & Strausberg, R. L. (2001). Genome and genetic resources from the cancer genome anatomy project. *Human Molecular Genetics*, *10*(7), 663-667.
- Roberts, R.M., Baumbach, G.A., Buhi, W.C., Denny, J. B., Fitzgerald, L.A., Babelyn, S.F., and Horst, M.N. (1984). Analysis of membrane polypeptides by two-dimensional polyacrylamide gel electrophoresis. *Molecular and Chemical Characterization of Membrane Receptors*. *3*, 61-113.
- Rosario, R., Araki, H., Print, C.G., & Shelling, A.N. (2012). The transcriptional targets of mutant FOXL2 in granulosa cell tumours. *PLoS One*, *7*(9), e46270.

- Rosario, R., Blenkiron, C., & Shelling, A. N. (2013). Comparative study of microRNA regulation on FOXL2 between adult-type and juvenile-type granulosa cell tumours in vitro. *Gynecologic Oncology*, *129*(1), 209-215.
- Schrader, K. A., Gorbacheva, B., Senz, J., Heravi-Moussavi, A., Melnyk, N., Salamanca, C., Maines-Bandiera, S., Cooke, S. L., Leung, P., Brenton, J. D., Gilks, C. B., Monahan, J., & Huntsman, D. (2009). The specificity of the FOXL2 c.402C>G somatic mutation: a survey of solid tumors. *PLoS One*, *4*(11), e7988.
- Sekido, R. & Lovell-Badge, R. (2012). Genetic control of testis development. *Sexual Development*, *7*, 21-32.
- Shah, S. P., Kobel, M., Senz, J., Morin, R. D., Clarke, B. A., Wiegand, K. C., . . . Huntsman, D. G. (2009). Mutation of FOXL2 in granulosa-cell tumors of the ovary. *The New England Journal of Medicine*, *360*(26), 2719-2729.
- She, Z. Y., & Yang, W. X. (2014). Molecular mechanisms involved in mammalian primary sex determination. *Journal of Molecular Endocrinology*, *53*(1), R21-R37.
- Smith, K. N., Halfyard, S. J., Yaskowiak, E. S., Shultz, K. L., Beamer, W. G., & Dorward, A. M. (2013). Fine map of the Gct1 spontaneous ovarian granulosa cell tumor locus. *Mammalian Genome*, *24*(1-2), 63-71.
- Tanaka, S.S. & Nishinakamura, R. (2014). Regulation of male sex determination: genital ridge formation and Sry activation in mice. *Cellular and Molecular Life Sciences*, *71*, 4781-4802.
- Tennent, B. J., Beamer, W. G., Shultz, L. D., & Adamson, E. D. (1989). Epidermal growth factor receptors in spontaneous ovarian granulosa cell tumors of SWR-derived mice. *International Journal of Cancer*, *44*(3), 477-482.
- Tennent, B. J., Shultz, K. L., Sundberg, J. P., & Beamer, W. G. (1990). Ovarian granulosa cell tumorigenesis in SWR-derived F1 hybrid mice; preneoplastic follicular abnormality and malignant disease progression. *American Journal of Obstetrics and Gynecology*, *163*(2), 625-634.
- Tennent, B. J., Shultz, K. L., & Beamer, W. G. (1993). Genetic susceptibility for C19 androgen induction of ovarian granulosa cell tumorigenesis in SWXJ strains of mice. *Cancer Research*, *53*(5), 1059-1063.
- Tingen, C., Kim, A., & Woodruff, T. K. (2009). The primordial pool of follicles and nest breakdown in mammalian ovaries. *Molecular Human Reproduction*, *15*(12), 795-803.
- Tomaselli, S., Megiorni, F., Lin, L., Mazzilli, M. C., Gerrelli, D., Majore, S., Grammatico, P., & Achermann, J. C. (2011). Human RSPO1-R-spondin1 is

- expressed during early ovary development and augments β -catenin signaling. *PLoS One*, 6(1), e16366.
- Uda, M., Ottolenghi, C., Crisponi, L., Garcia, J. E., Deiana, M., Kimber, W., . . . Pilia, G. (2004). Foxl2 disruption causes mouse ovarian failure by pervasive blockage of follicle development. *Human Molecular Genetics*, 13(11), 1171-1181.
- Uhlenhaut, N. H., Jakob, S., Anlag, K., Eisenberger, T., Sekido, R., Kress, J., . . . Treier, M. (2009). Somatic sex reprogramming of adult ovaries to testes by FOXL2 ablation. *Cell*, 139(6), 1130-1142.
- Vadakkadath Meethal, S., & Atwood, C. S. (2005). The role of hypothalamic-pituitary-gonadal hormones in the normal structure and functioning of the brain. *Cellular and Molecular Life Sciences : CMLS*, 62(3), 257-270.
- Van Den Berg-Bakker, C. A. M., Hagemeyer, A., Franken-Postma, E. M., Smit, V. T. H. B. M., Kuppen, P. J. K., Van Ravenswaay Claasen, H. H., . . . Schrier, P. I. (1993). Establishment and characterization of 7 ovarian carcinoma cell lines and one granulosa tumor cell line: Growth features and cytogenetics. *International Journal of Cancer*, 53(4), 613-620.
- Wallace, W. H., & Kelsey, T. W. (2010). Human ovarian reserve from conception to the menopause. *PloS One*, 5(1), e8772.
- Wilhelm, D., Palmer, S., & Koopman, P. (2007). Sex determination and gonadal development in mammals. *Physiological Reviews*, 87(1), 1-28.
- Windley, S. P., & Wilhelm, D. (2015). Signaling pathways involved in mammalian sex determination and gonad development. *Sexual Development*, 9(6), 297-315.
- Wunsch, L., & Schober, J. M. (2007). Imaging and examination strategies of normal male and female sex development and anatomy. *Best Practice & Research. Clinical Endocrinology & Metabolism*, 21(3), 367-379.
- Young, R. H., Dickersin, G. R., & Scully, R. E. (1984). Juvenile granulosa cell tumor of the ovary. A clinicopathological analysis of 125 cases. *The American Journal of Surgical Pathology*, 8(8), 575-596.
- Zhang, H., Vollmer, M., De Geyter, M., Litzistorf, Y., Ladewig, A., Dürrenberger, M., . . . De Geyter, C. (2000). Characterization of an immortalized human granulosa cell line (COV434). *Molecular Human Reproduction*, 6(2), 146-153.
- Zheng, W., Zhang, H., Gorre, N., Risal, S., Shen, Y. & Liu, K. (2014). Two classes of ovarian primordial follicles exhibit distinct developmental dynamics and physiological functions. *Human Molecular Genetics*, 23 (4), 920-928.

Appendix A Copyright Permissions



Permissions Department
Contracts, Copyrights and Permissions
Segment Administration

PERMISSION LICENSE: PRINT REPUBLICATION

Request ID/Invoice Number: CLA18040

Date: August 25, 2014

To: Clare Lewis
5357, Health Sciences Centre
Memorial University of Newfoundland
300 Prince Phillip Drive
St. Johns NL A1B 3V6
CANADA
"Licensee"

McGraw-Hill Education Material

Author: Mescher, Anthony
Title: Junqueira's Basic Histology: Text and Atlas, 13/e © 2013
ISBN: 0071780335
Description of material: Figure 22-2, pg. 451 (ONLY)

Fee: WAIVED

Licensee Work:

Author: Clare Lewis
Title: characterization of spontaneous, juvenile-type granulosa cell tumours from SWR mice
Publisher: Memorial University of Newfoundland [Thesis]
Publication Date: 2014
Print Run: 3
Distribution Territory: Canada
Languages: English

Permission for the use described above is granted under the following conditions:

1. The permission fee is waived.

Request ID/Invoice Number: CLA18040

2. No adaptations, deletions, or changes will be made in the material without the prior written consent of McGraw-Hill Education.
3. This permission is non-exclusive, non-transferable, and limited to the use specified herein. McGraw-Hill Education expressly reserves all rights in this material.
4. A credit line must be printed on the first page on which the material appears. This credit must include the author, title, copyright date, and publisher, and indicate that the material is reproduced with permission of McGraw-Hill Education.
5. This permission does not allow the use of any material, including but not limited to photographs, charts, and other illustrations, which appears in a McGraw-Hill Education work copyrighted in or credited to the name of any person or entity other than McGraw-Hill Education. Should you desire permission to use such material, you must seek permission directly from the owner of that material, and if you use such material you agree to indemnify McGraw-Hill Education against any claim from the owners of that material.

Please sign and return one copy (with payment, if applicable) to the address above, as outlined in Clause 1 of this agreement.

For McGraw-Hill Education:

Ebony Lane
Permissions Department
McGraw-Hill Education

For Licensee:

Name  _____
DocuSigned by:
Clare Lewis
0766AE76E06A42D

Title Master's Candidate

Request ID/Invoice Number: CLA18040

**BIOSCIENTIFICA LTD. LICENSE
TERMS AND CONDITIONS**

Jun 30, 2016

This Agreement between Clare Lewis ("You") and BioScientifica Ltd. ("BioScientifica Ltd.") consists of your license details and the terms and conditions provided by BioScientifica Ltd. and Copyright Clearance Center.

The publisher has provided special terms related to this request that can be found at the end of the Publisher's Terms and Conditions.

All payments must be made in full to CCC. For payment instructions, please see information listed at the bottom of this form.

License Number	3656160125683
License date	Jun 25, 2015
Licensed Content Publisher	BioScientifica Ltd.
Licensed Content Publication	Journal of Molecular Endocrinology
Licensed Content Title	FOXL2: a central transcription factor of the ovary
Licensed Content Author	Adrien Georges, Aurelie Auguste, Laurianne Bessi�re et al.
Licensed Content Date	Feb 1, 2014
Licensed Content Volume Number	52
Licensed Content Issue Number	1
Type of Use	Thesis/Dissertation
Requestor type	Academic institution
Format	Print, Electronic
Portion	chart/graph/table/figure
Number of charts/graphs/tables/figures	1
Rights for	Main product
Duration of use	Life of current edition
Creation of copies for the disabled	no
With minor editing privileges	no
For distribution to	Worldwide
In the following language(s)	Original language of publication
With incidental promotional use	no
The lifetime unit quantity of new product	0 to 499
The requesting person/organization is:	Clare Lewis/Memorial University of Newfoundland
Order reference number	
Title of your thesis / dissertation	Characterization of spontaneous, juvenile-type granulosa cell tumours from SWR mice

Appendix B Summary of inventoried samples

Table B.1 Summary of normal ovarian samples from SWR background mice analyzed by immunoblotting.

Normal (N) Reference ID	Strain	Animal ID #	Date of Birth	Date of Necropsy
22	SWR x SWR.CAST-X1 (F1)	22099	07/05/13	08/19/13
23	SWR x SWR.CAST-X1 (F1)	22142	08/05/13	09/16/13
24	SWR x SWR.CAST-X1 (F1)	22143	08/05/13	09/16/13
25	SWR x SWR.CAST-X1 (F1)	22158	08/20/13	10/03/13
26	SWR x SWR.CAST-X1 (F1)	22159	08/20/13	10/03/13
31	SWR x SWR.CAST-X1 (F1)	22190	09/11/13	10/23/13
32	SWR x SWR.CAST-X1 (F1)	22191	09/11/13	10/23/13
33	SWR x SWR.CAST-X1 (F1)	22192	09/11/13	10/23/13
37	SWR x SWR.CAST-X1 (F1)	22174	09/02/13	10/15/13
38	SWR x SWR.CAST-X1 (F1)	22175	09/02/13	10/15/13
39	SWR x SWR.CAST-X1 (F1)	22176	09/02/13	10/15/13
40	SWR x SWR.CAST-X1 (F1)	22177	09/02/13	10/15/13
41	SWR x SWR.CAST-X1 (F1)	22178	09/02/13	10/15/13
42	SWR x SWR.CAST-X1 (F1)	22470	04/16/14	06/25/14
43	SWR x SWR.CAST-X1 (F1)	22471	04/16/14	06/25/14
44	SWR x SWR.CAST-X1 (F1)	22472	04/16/14	06/25/14
45	SWR x SWR.CAST-X1 (F1)	22473	04/16/14	06/25/14
46	SWR x SWR.CAST-X1 (F1)	22489	05/01/14	06/25/14
47	SWR x SWR.CAST-X1 (F1)	22493	05/01/14	06/25/14
48	SWR x SWR.CAST-X1 (F1)	22491	05/01/14	06/25/14
49	SWR x SWR.CAST-X1 (F1)	22492	05/01/14	06/25/14

Table B.2 Summary of GCT samples from SWR background mice analyzed by immunoblotting.

GCT (T) Reference ID	Strain	Animal ID #	Date of Birth	Date of Necropsy
1	SWR x SWR.CAST-X1 (F1)	22100	07/05/13	08/19/13
3	SWR x SWR.CAST-X1 (F1)	21875	01/04/13	02/18/13
4	SWR x SWR.CAST-X1 (F1)	21876	01/04/13	02/18/13
11	SWR. CAST-X1	22094	06/30/13	09/02/13
12	SWR. CAST-X1	22140	07/29/13	09/09/13
13	SWR x SWR.CAST-X1 (F1)	21976	03/28/13	05/13/13
14	SWR x SWR.CAST-X1 (F1)	21977	03/28/13	05/13/13
15	SWR x SWR.CAST-X1 (F1)	21978	03/28/13	05/13/13
17	SWR. CAST-X1	22092	06/30/13	09/02/13
21	SWR x SWR.CAST-X1 (F1)	22227	09/24/13	11/08/13
24	SWR x SWR.CAST-X1 (F1)	22309	11/16/13	01/09/14
25	SWR x SWR.CAST-X1 (F1)	22313	11/16/13	01/10/14
27	SWR x SWR.CAST-X1 (F1)	22297	11/16/13	01/10/14
28	SWR x SWR.CAST-X1 (F1)	22488	05/01/14	06/25/14
29	SWR x SWR.CAST-X1 (F1)	22490	05/01/14	06/25/14

Table B.3 Summary of cell lysate samples from the human cell line COV434 analyzed by immunoblotting.

COV434 (C) Reference ID	Passage #
1	27
2	27
3	27
4	27
5	27
6	27
7	4
8	4
9	4

Table B.4 Summary of tissues from mice for analysis by IHC.

Tissue Type	Tissue Treatment
Testis	Untreated
Normal Ovary	DHEA-treated
GCT	DHEA-treated
GCT	DHEA-treated